Title
Measurement of top quark pair production in association with a Z boson in proton-proton collisions at s = 13 TeV

Journal
Journal of High Energy Physics, 2020(3)

ISSN
1126-6708

Authors
Sirunyan, AM
Tumasyan, A
Adam, W
et al.

Publication Date
2020-03-01

DOI
10.1007/jhep03(2020)056

Peer reviewed

EUROPEAN ORGANIZATION FOR NUCLEAR RESEARCH (CERN)

CERN-EP-2019-124
2020/03/23

CMS-TOP-18-009

Measurement of top quark pair production in association with a Z boson in proton-proton collisions at $\sqrt{s} = 13\,\text{TeV}$

The CMS Collaboration*

Abstract

A measurement of the inclusive cross section of top quark pair production in association with a Z boson using proton-proton collisions at a center-of-mass energy of 13 TeV at the LHC is performed. The data sample corresponds to an integrated luminosity of $77.5\,\text{fb}^{-1}$, collected by the CMS experiment during 2016 and 2017. The measurement is performed using final states containing three or four charged leptons (electrons or muons), and the Z boson is detected through its decay to an oppositely charged lepton pair. The production cross section is measured to be $\sigma(\mathrm{t\bar{t}Z}) = 0.95 \pm 0.05\,(\text{stat}) \pm 0.06\,(\text{syst})\,\text{pb}$. For the first time, differential cross sections are measured as functions of the transverse momentum of the Z boson and the angular distribution of the negatively charged lepton from the Z boson decay. The most stringent direct limits to date on the anomalous couplings of the top quark to the Z boson are presented, including constraints on the Wilson coefficients in the framework of the standard model effective field theory.

"Published in the Journal of High Energy Physics as `doi:10.1007/JHEP03(2020)056`."

*See Appendix A for the list of collaboration members

1 Introduction

The large amount of proton-proton (pp) collision data at a center-of-mass energy of 13 TeV at the CERN LHC allows for precision measurements of standard model (SM) processes with very small production rates. Precise measurements of the inclusive and differential cross sections of the $\mathrm{t\bar{t}Z}$ process are of particular interest because it can receive sizable contributions from phenomena beyond the SM (BSM) [1, 2]. The $\mathrm{t\bar{t}Z}$ production is the most sensitive process for directly measuring the coupling of the top quark to the Z boson. Also, this process is an important background to several searches for BSM phenomena, as well as to measurements of certain SM processes, such as $\mathrm{t\bar{t}}$ production in association with the Higgs boson ($\mathrm{t\bar{t}H}$).

The inclusive cross section for $\mathrm{t\bar{t}Z}$ production has been measured by both the CMS and ATLAS Collaborations using pp collision data at $\sqrt{s} = 13\,\mathrm{TeV}$, corresponding to an integrated luminosity of about $36\,\mathrm{fb}^{-1}$. The CMS Collaboration used events containing three or four charged leptons (muons or electrons) collected in 2016 and reported a value $\sigma(\mathrm{t\bar{t}Z}) = 0.99^{+0.09}_{-0.08}\,(\mathrm{stat})\,^{+0.12}_{-0.10}\,(\mathrm{syst})\,\mathrm{pb}$ [3]. The ATLAS Collaboration used events with two, three, or four charged leptons in a data sample collected in 2015 and 2016 and measured $\sigma(\mathrm{t\bar{t}Z}) = 0.95 \pm 0.08\,(\mathrm{stat}) \pm 0.10\,(\mathrm{syst})\,\mathrm{pb}$ [4].

In this paper, we report an updated measurement of the $\mathrm{t\bar{t}Z}$ cross section in three- and four-lepton final states using pp collision data collected with the CMS detector in 2016 and 2017, corresponding to a total integrated luminosity of $77.5\,\mathrm{fb}^{-1}$. The Z boson is detected through its decay to an oppositely charged lepton pair. While the data analysis strategy remains similar to the one presented in Ref. [3], this new measurement benefits largely from an improved lepton selection procedure based on multivariate analysis techniques and a more inclusive trigger selection. In addition to the inclusive cross section, the differential cross section is measured as a function of the transverse momentum of the Z boson, $p_{\mathrm{T}}(\mathrm{Z})$, and $\cos\theta^*_{\mathrm{Z}}$. The latter observable is the cosine of the angle between the direction of the Z boson in the detector reference frame and the direction of the negatively charged lepton in the rest frame of the Z boson.

Because of the key role of the top quark interaction with the Z boson in many BSM models [5–10], the differential cross section measurements can be used to constrain anomalous $\mathrm{t\bar{t}Z}$ couplings. To this end, we pursue two different interpretations. A Lagrangian containing anomalous couplings [11] is used to obtain bounds on the vector and axial-vector currents, as well as on the electroweak magnetic and electric dipole moments of the top quark. The interpretation is extended in the context of SM effective field theory (SMEFT) [12], and we constrain the Wilson coefficients of the relevant BSM operators of mass dimension 6. There are 59 operators, among which we select the four most relevant linear combinations, as described in Ref. [13].

This paper is organized as follows. In Section 2, a brief description of the CMS detector is provided. In Section 3, the simulation of signal and background processes is discussed, followed by the description of the selection of events online (during data taking) and offline (after data taking) in Section 4. The background estimation is discussed in Section 5, and the sources of systematic uncertainties that affect the measurements are discussed in Section 6. In Section 7, we present the results of the inclusive and differential measurements, followed by the limits on anomalous couplings and SMEFT interpretation. The results are summarized in Section 8.

2 The CMS detector

The central feature of the CMS apparatus is a superconducting solenoid of 6 m internal diameter, providing a magnetic field of 3.8 T. Within the solenoid volume are a silicon pixel and strip tracker, a lead tungstate crystal electromagnetic calorimeter (ECAL), and a brass and scintillator hadron calorimeter, each composed of a barrel and two endcap sections. Forward calorimeters extend the pseudorapidity (η) coverage. Muons are detected in gas-ionization chambers embedded in the steel magnetic flux-return yoke outside the solenoid. Events of interest are selected using a two-tiered trigger system [14]. The first level, composed of custom hardware processors, uses information from the calorimeters and muon detectors to select events, while the second level selects events by running a version of the full event reconstruction software optimized for fast processing on a farm of computer processors. A more detailed description of the CMS detector, together with a definition of the coordinate system used and the relevant kinematic variables, can be found in Ref. [15].

3 Data samples and object selection

The data sample used in this measurement corresponds to an integrated luminosity of $77.5\,\mathrm{fb}^{-1}$ of pp collision events collected with the CMS detector during 2016 and 2017. To incorporate the LHC running conditions and the CMS detector performance, the two data sets were analyzed independently with appropriate calibrations applied, and combined at the final stage to extract the cross section value, as described in more detail in Section 6.

Simulated Monte Carlo (MC) events are used to model the signal selection efficiency, to test the background prediction techniques, and to predict some of the background yields. Two sets of simulated events for each process are used in order to match the different data-taking conditions in 2016 and 2017. Events for the $\mathrm{t\bar{t}Z}$ signal process and a variety of background processes, including production of WZ and triple vector boson (VVV) events, are simulated at next-to-leading order (NLO) in perturbative quantum chromodynamics (QCD) using the MADGRAPH5_aMC@NLO v2.3.3 and v2.4.2 generators [16]. In these simulations, up to one additional jet is included in the matrix element calculation. The NLO POWHEG v2 [17] generator is used for simulation of the $\mathrm{t\bar{t}}$ production process, as well as for processes involving the Higgs boson produced in vector boson fusion (VBF) or in association with vector bosons or top quarks. The NNPDF3.0 (NNPDF3.1) [18, 19] parton distribution functions (PDFs) are used for simulating the hard process. Table 1 gives an overview of the event generators, PDF sets, and cross section calculations that are used for the signal and background processes. For all processes, the parton showering and hadronization are simulated using PYTHIA 8.203 [20, 21]. The modeling of the underlying event is done using the CUETP8M1 [22, 23] and CP5 tunes [24] for simulated samples corresponding to the 2016 and 2017 data sets, respectively. The CUETP8M2 and CUETP8M2T4 tunes [25] are used for the 2016 $\mathrm{t\bar{t}H}$ and $\mathrm{t\bar{t}VV}$ samples, respectively. Double counting of the partons generated with MADGRAPH5_aMC@NLO and PYTHIA is removed using the FXFX [26] matching schemes for NLO samples.

The $\mathrm{t\bar{t}Z}$ cross section measurement is performed in a phase space defined by the invariant mass of an oppositely charged and same-flavor lepton pair $70 \leq m(\ell\ell) \leq 110\,\mathrm{GeV}$. Using a simulated signal sample, the contribution of $\mathrm{t\bar{t}}\gamma^*$ was verified to be negligible. The Z boson branching fractions to charged and neutral lepton pairs are set to $(\mathrm{Z} \rightarrow \ell\ell, \nu\nu) = 0.301$ [27]. The theoretical prediction of the inclusive $\mathrm{t\bar{t}Z}$ cross section is computed for $\sqrt{s} = 13\,\mathrm{TeV}$ at NLO in QCD and electroweak accuracy using MADGRAPH5_aMC@NLO and the PDF4LHC recommendations [28] to assess the uncertainties. It is found to be $0.84 \pm 0.10\,\mathrm{pb}$ [29–31], with the renormalization and factorization scales μ_F and μ_R set to $\mu_R = \mu_F = m(\mathrm{t}) + m(\mathrm{Z})/2$, where $m(\mathrm{t}) = 172.5\,\mathrm{GeV}$ is the on-shell top quark mass [29].

All events are processed through a simulation of the CMS detector based on GEANT4 [41] and

Table 1: Event generators used to simulate events for the various processes. For each of the simulated processes shown, the order of the cross section normalization, the event generator used, the perturbative order of the generator calculation, and the NNPDF versions at NLO and at next-to-next-to-leading order (NNLO) used in simulating samples for the 2016 (2017) data sets.

Process	Cross section normalization	Event generator	Perturbative order	NNPDF version
$\mathrm{t\bar{t}Z}$, tZq, $\mathrm{t\bar{t}W}$, WZ, Z+jets, VVV, $\mathrm{t\bar{t}}\gamma^{(*)}$, $\mathrm{W}\gamma^{(*)}$, $\mathrm{Z}\gamma^{(*)}$	NLO	MADGRAPH5_aMC@NLO v2.2.3 (v2.4.2)	NLO	3.0 NLO (3.1 NNLO)
$\mathrm{gg} \to \mathrm{ZZ}$	NLO [32]	MCFM v7.0.1 [33] JHUGEN v7.0.11 [34]	LO	3.0 LO (3.1LO)
$\mathrm{q\bar{q}} \to \mathrm{ZZ}$	NNLO [35]	POWHEG v2 [36, 37]	NLO	3.0 NLO (3.1 NNLO)
WH, ZH	NLO	POWHEG v2 MINLO HVJ [38] JHUGEN v7.0.11 [34]	NLO	3.0 NLO (3.1 NNLO)
VBF H	NLO	POWHEG v2	NLO	3.0 NLO (3.1 NNLO)
$\mathrm{t\bar{t}H}$	NLO	POWHEG v2 [39]	NLO	3.0 NLO (3.1 NNLO)
$\mathrm{t\bar{t}}$	NNLO+NNLL [40]	POWHEG v2	NLO	3.0 NLO (3.1 NNLO)
$\mathrm{t\bar{t}VV}$, tHW, tHq, tWZ	LO	MADGRAPH5_aMC@NLO	LO	3.0 LO (3.1 NNLO)

are reconstructed with the same algorithms as used for data. Minimum-bias pp interactions occuring in the same or nearby bunch crossing, referred to as pileup (PU), are also simulated, and the observed distribution of the reconstructed pp interaction vertices in an event is used to ensure that the simulation describes the data. The CMS particle-flow (PF) algorithm [42] is used for particle reconstruction and identification, yielding a consistent set of electron [43], muon [44], charged and neutral hadron, and photon candidates. These particles are defined with respect to the primary IV (PV), chosen to have the largest value of summed physics-object p_{T}^2, where these physics objects are reconstructed by a jet-finding algorithm [45, 46] applied to all charged tracks associated with the vertex. Jets are reconstructed by clustering PF candidates using the anti-k_{T} algorithm [45] with a distance parameter $R = 0.4$. The influence of PU is mitigated through a charged hadron subtraction technique, which removes the energy of charged hadrons not originating from the PV [47]. Jets are calibrated separately in simulation and data, accounting for energy deposits of neutral particles from PU and any nonlinear detector response [48, 49]. Jets with $p_{\mathrm{T}} > 30\,\mathrm{GeV}$ and $|\eta| < 2.4$ are selected for the analysis. Jets are identified as originating from the hadronization of b quarks using the DEEPCSV algorithm [50]. This algorithm achieves an averaged efficiency of 70% for b quark jets to be correctly identified, with a misidentification rate of 12% for charm quark jets and 1% for jets originating from u, d, s quarks or gluons.

Lepton identification and selection are critical ingredients in this measurement. Prompt leptons are those originating from direct W or Z boson decays, while nonprompt are those that are either misidentified jets or genuine leptons resulting from semileptonic decays of hadrons containing heavy-flavor quarks. To achieve an effective rejection of the nonprompt leptons, a multivariate analysis has been developed separately for electrons and muons similar to the one presented in Ref. [51]. A boosted decision tree (BDT) classifier is used via the TMVA toolkit [52] for the multivariate analysis. In addition to the lepton p_{T} and $|\eta|$, the training uses several discriminating variables. These comprise the kinematic properties of the jet closest to the lepton; the impact parameter in the transverse plane of the lepton track with respect to the PV; a variable that quantifies the quality of the geometric matching of the track in the silicon tracker with the signals measured in the muon chambers; variables related to the ECAL shower shape of electrons; two variants of relative isolation—one computed with a fixed ($R = 0.3$) and another with a variable cone size depending on the lepton p_T [53]. The relative isolation is defined as the scalar p_T sum of the particles within a cone around the lepton direction, divided by the lepton p_T. Comparing a stringent requirement on the BDT output to the non-BDT-based lepton identification used in Ref. [3], an increase of up to 15% in prompt lepton selection efficiency is achieved, while the nonprompt lepton selection efficiency is reduced by about a factor 2 to 4, depending on the lepton p_T. Muons (electrons) passing the BDT selection and having $p_T > 10\,\text{GeV}$ and $|\eta| < 2.4$ (2.5) are selected. The efficiency for prompt leptons in the $\mathrm{t\bar{t}Z}$ signal events in the three lepton channel is around 90% when averaged over p_T range used in the analysis for both electrons and muons. In the four-lepton channel, a less stringent lepton selection is used and it results in an average efficiency of 95%. In order to avoid double counting, jets within a cone of $\Delta R = \sqrt{(\Delta\eta)^2 + (\Delta\phi)^2} = 0.4$ around the selected leptons are discarded, where $\Delta\eta$ and $\Delta\phi$ are the differences in pseudorapidity and azimuthal angle, respectively.

4 Event selection and observables

Events are selected using a suite of triggers each of which requires the presence of one, two, or three leptons. For events selected by the triggers that require at least one muon or electron, the p_T threshold for muons (electrons) was 24 (27) GeV during 2016 and 27 (32) GeV in 2017. For triggers that require the presence of at least two leptons, the p_T thresholds are 23 and 17 GeV for the highest p_T (leading) and 12 and 8 GeV for the second-highest p_T (subleading) electron and muon, respectively. This strategy ensures an overall trigger efficiency higher than 98% for events passing the lepton selection described below over the entire 2016 and 2017 data sets. These efficiencies are measured in data samples with an independent trigger selection and compared to those obtained in simulation. The measured differences are mitigated by reweighting the simulation by appropriate factors that differ from unity by less than 2 (3)% in the 2016 (2017) data set.

Events with exactly three leptons ($\mu\mu\mu$, $\mu\mu$e, μee, or eee) satisfying $p_T > 40, 20, 10\,\text{GeV}$ or exactly four leptons ($\mu\mu\mu\mu$, $\mu\mu\mu$e, $\mu\mu$ee, μeee, or eeee) with $p_T > 40$, 10, 10, 10 GeV are analyzed separately. In both categories, exactly one oppositely charged and same-flavor lepton pair consistent with the Z boson hypothesis is required, namely, for the three- and four-lepton categories $|m(\ell\ell) - m(\mathrm{Z})| < 10$ and 20 GeV, respectively. This selection reduces the contributions from background events with zero or more than one Z boson. Events containing zero jets are rejected. The measurement uses the jet multiplicity N_j in different event categories depending on the number of b-tagged jets N_b in the event. For the three-lepton channel these are $N_b = 0, 1, \geq 2$, while for the four-lepton channel these categories are limited to $N_b = 0, \geq 1$. The analysis makes use of several control regions in data to validate the background predictions, as well as to control the systematic uncertainties associated with them. The details are given in Section 5.

5 Background predictions

Several SM processes contribute to the three- and four-lepton final states. The $\mathrm{t\bar{t}Z}$ process typically produces events with large jet and b-tagged jet multiplicities. In contrast, events with $N_b = 0$ are dominated by background processes. Following closely the methodologies used in Ref. [3], the separation between signal and backgrounds is obtained from a binned maximum-likelihood fit with nuisance parameters. In the fit, the contributions from the various background processes are allowed to vary within their uncertainties.

The main contributions to the background arise from processes with at least one top quark produced in association with a W, Z, or Higgs boson, i.e., $\mathrm{t\bar{t}H}$, $\mathrm{t\bar{t}W}$, tWZ, tZq, tHq, tHW, $\mathrm{t\bar{t}VV}$, and $\mathrm{t\bar{t}t\bar{t}}$. They are collectively denoted as $\mathrm{t(\bar{t})X}$ and estimated using simulated samples. We consider both the theoretical and experimental systematic uncertainties in the background yields for the $\mathrm{t(\bar{t})X}$ category. The theoretical uncertainty in the inclusive cross section is evaluated by varying μ_R and μ_F in the matrix element and parton shower description by a factor of 2 up and down, ignoring the anticorrelated variations, as well as the uncertainties stemming from the choice of PDFs. For each of these processes, this uncertainty is found to be not larger than 11% [16, 30, 54]. Among them, the tZq cross section was recently measured by the CMS Collaboration with a precision of 15% [55]. Thus, we use this measurement and its uncertainty for the tZq cross section, and 11% as uncertainty for the normalization of the other processes.

The WZ production constitutes the second-largest background contribution, in particular for events with three leptons, while in the four-lepton category, ZZ production becomes substantial. For both these processes, the prediction of the overall production rate and the relevant kinematic distributions can be validated in data samples that do not overlap with the signal region. Events with three leptons, two of which form a same-flavor pair with opposite charge and satisfy $|m(\ell\ell) - m(\mathrm{Z})| < 10\,\mathrm{GeV}$ and $N_\mathrm{b} = 0$, are used to validate the WZ background prediction. Four-lepton events with two Z boson candidates are used to constrain the uncertainties in the prediction of the ZZ yield.

Figure 1 presents the observed and predicted event yields for these categories and the reconstructed transverse momentum of the Z boson candidates, as well as the lepton flavor and N_b in the ZZ-enriched control region. Agreement within the systematic uncertainties is observed. A normalization uncertainty of 10% is assigned to the prediction of the WZ and ZZ backgrounds [56, 57], and an additional 20% uncertainty is appended to the WZ background prediction with $N_\mathrm{j} \geq 3$ because of the observed discrepancy in events with high jet multiplicity.

We also estimate the potential mismodeling of WZ production when heavy-quark pairs from gluon splitting are included by using a control data sample containing a Z boson candidate and two b-tagged jets. The distribution of the angle between the two b jets is sensitive to the modeling of gluon splitting and good agreement is observed. A systematic uncertainty of 20% is estimated from possible mismodeling. Taking into account the fraction of simulated WZ events with gluon splitting, the additional uncertainty in the prediction of WZ events with $N_\mathrm{b} \geq 1$ is estimated to be 8%.

The background with nonprompt leptons mainly originates from $\mathrm{t\bar{t}}$ or $\mathrm{Z} \to \ell\ell$ events in which a nonprompt lepton arises from a semileptonic decay of a heavy-flavor hadron or misidentified jets in addition to two prompt leptons. The lepton selection specifically targets the reduction of nonprompt-lepton backgrounds to a subdominant level, while keeping the signal efficiency high. The details of the nonprompt-lepton background estimation are given in Ref. [3]. In this analysis, it is validated in simulation and with a data control sample that contains three-lepton events without a Z boson candidate. Figure 2 shows the predicted and observed yields in this control sample for different lepton flavors, as a function of the p_T of the lowest-p_T lepton and N_b. We find good agreement between predicted and observed yields. Based on these studies, a systematic uncertainty of 30% in the prediction of the background with nonprompt leptons is assigned, while the statistical uncertainty ranges between 5–50%, depending on the measurement bin.

A small contribution to the background comes from VVV processes. We group them in the "rare" category as these have relatively small production rates. Processes that involve a photon ($\mathrm{Z}\gamma^{(*)}$ and $\mathrm{t\bar{t}}\gamma$) are denoted by $\mathrm{X}\gamma$. The contribution from both of these categories to the selected event count is evaluated using simulated samples described in Section 3. As in the

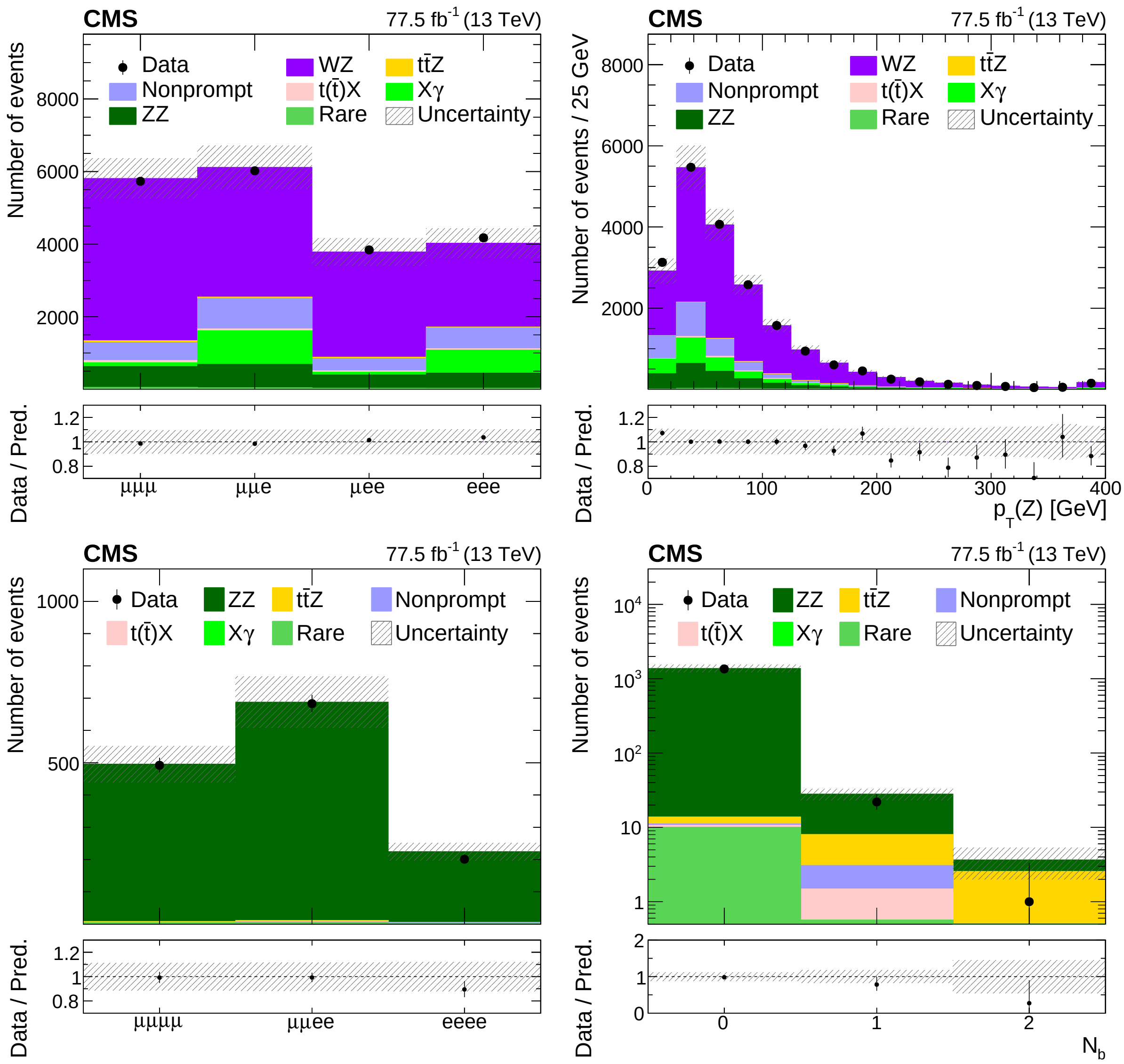

Figure 1: The observed (points) and predicted (shaded histograms) event yields versus lepton flavor (upper left), and the reconstructed transverse momentum of the Z boson candidates (upper right) in the WZ-enriched data control event category, and versus lepton flavor (lower left) and N_b (lower right) in the ZZ-enriched event category. The vertical lines on the points show the statistical uncertainties in the data, and the band the total uncertainty in the predictions. The lower panels show the ratio of the event yields in data to the predictions.

case of the $\mathrm{t}(\bar{\mathrm{t}})\mathrm{X}$ backgrounds, scale factors are applied to account for small differences between data and simulation in trigger selection, lepton identification, jet energy corrections, and b jet selection efficiency. The overall uncertainty in the normalization of the rare background category is estimated to be 50% [29, 58], while for $\mathrm{X}\gamma$ it is 20% [59, 60]. The statistical uncertainty stemming from the finite size of the simulated background samples are typically small, around 5% and reaching 100% only in the highest jet multiplicity regions. The simulation of photon conversion is validated in a data sample with three-lepton events where the invariant mass of the three leptons is required to be consistent with the Z boson mass. Good agreement between data and simulation is observed.

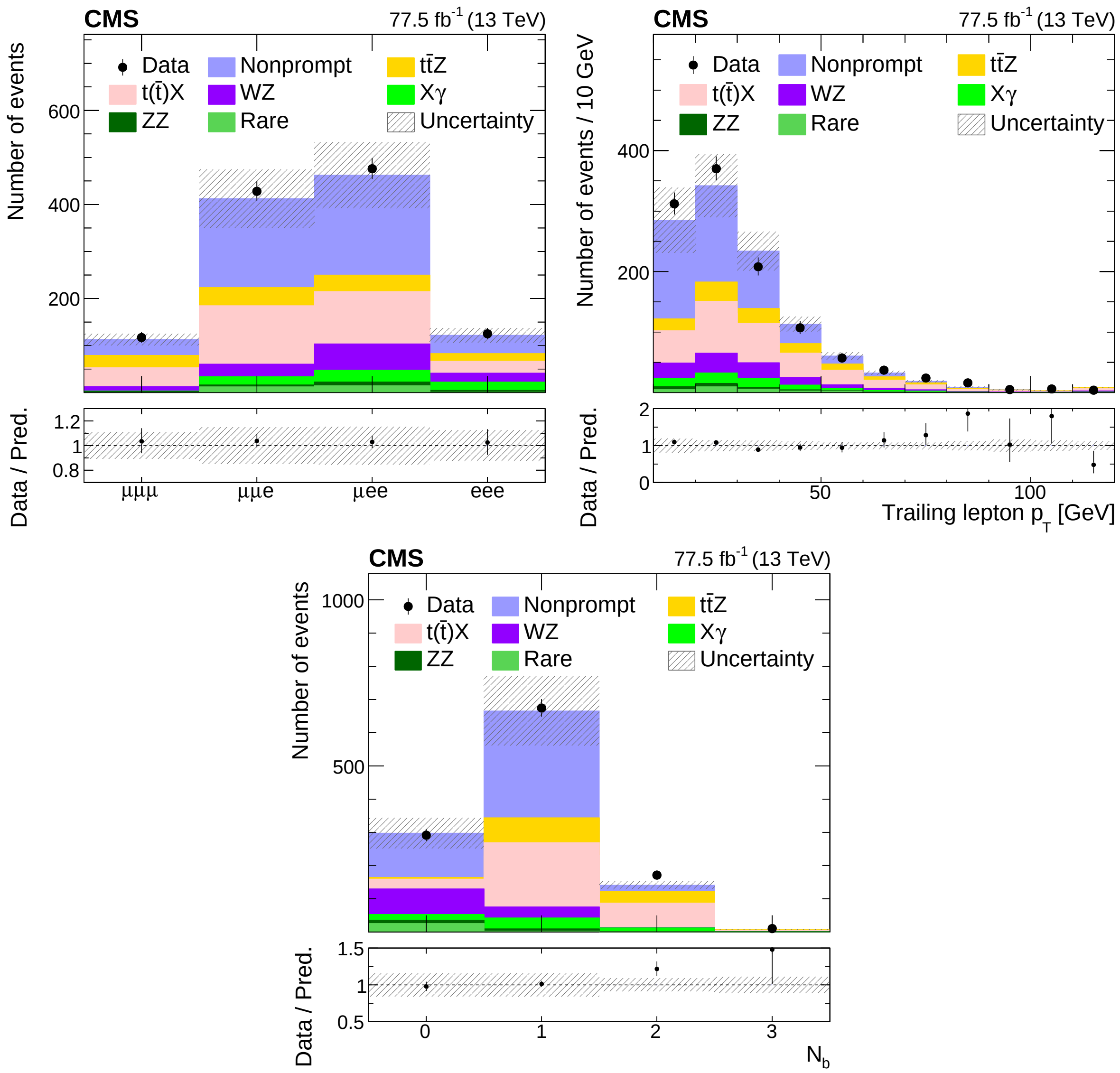

Figure 2: The observed (points) and predicted (shaded histograms) event yields in regions enriched with nonprompt lepton backgrounds in $t\bar{t}$-like processes as a function of the lepton flavors (upper left), the p_T of the lowest-p_T (trailing) lepton (upper right), and N_b (bottom). The vertical lines on the points show the statistical uncertainties in the data, and the band the total uncertainty in the predictions. The lower panels show the ratio of the event yields in data to the background predictions.

6 Systematic uncertainties

The systematic uncertainties affecting the signal selection efficiency and background yields are summarized in Table 2. The table shows the range of variations in the different bins of the analysis caused by each systematic uncertainty on the signal and background yields, as well as an estimate of the impact of each input uncertainty on the measured cross section.

The table also indicates whether the uncertainties are treated as uncorrelated or fully correlated between the 2016 and 2017 data sets.

The uncertainty in the integrated luminosity measurement in the 2016 (2017) data set is 2.5 (2.3)% [61, 62], and is uncorrelated between the two data sets. Simulated events are reweighted

Table 2: Summary of the sources, magnitudes, treatments, and effects of the systematic uncertainties in the final $\mathrm{t\bar{t}Z}$ cross section measurement. The first column indicates the source of the uncertainty, the second column shows the corresponding input uncertainty range for each background source and the signal. The third column indicates how correlations are treated between the uncertainties in the 2016 and 2017 data, where ✓ means fully correlated and × uncorrelated. The last column gives the corresponding systematic uncertainty in the $\mathrm{t\bar{t}Z}$ cross section using the fit result. The total systematic uncertainty, the statistical uncertainty and the total uncertainty in the $\mathrm{t\bar{t}Z}$ cross section are shown in the last three lines.

Source	Uncertainty range (%)	Correlated between 2016 and 2017	Impact on the $\mathrm{t\bar{t}Z}$ cross section (%)
Integrated luminosity	2.5	×	2
PU modeling	1–2	✓	1
Trigger	2	×	2
Lepton ID efficiency	4.5–6	✓	4
Jet energy scale	1–9	✓	2
Jet energy resolution	0–1	✓	<1
b tagging light flavor	0–4	×	<1
b tagging heavy flavor	1–4	×	2
Choice in μ_R and μ_F	1–4	✓	1
PDF choice	1–2	✓	<1
Color reconnection	1.5	✓	1
Parton shower	1–8	✓	<1
WZ cross section	10	✓	3
WZ high jet multiplicity	20	✓	1
WZ + heavy flavor	8	✓	1
ZZ cross section	10	✓	1
$\mathrm{t(\bar{t})X}$ background	10–15	✓	2
$\mathrm{X}\gamma$ background	20	✓	1
Nonprompt background	30	✓	1
Rare SM background	50	✓	1
Stat. unc. in nonprompt bkg.	5–50	×	<1
Stat. unc. in rare SM bkg.	5–100	×	<1
Total systematic uncertainty			6
Statistical uncertainty			5
Total			8

according to the distribution of the number of interactions in each bunch crossing corresponding to a total inelastic pp cross section of 69.2 mb [63]. The uncertainty in the latter, which affects the PU estimate, is 5% [64] and leads to about 2% uncertainty in the expected yields.

The uncertainties in the corrections to the trigger selection efficiencies are propagated to the results. A 2% uncertainty is assigned to the yields obtained in simulation. Lepton selection efficiencies are measured using a "tag-and-probe" method [43, 44] in bins of lepton p_{T} and η, and are found to be higher than 60 (95)% for lepton $p_{\mathrm{T}} \leq 25$ (> 25) GeV. These measurements are performed separately in data and simulation. The differences between these two measurements are used to scale the yields obtained in the simulation. They are typically around 1% and reach 10% for leptons with $p_{\mathrm{T}} < 20$ GeV. The systematic uncertainties related to this source vary between 4.5 and 6% in the signal and background yields.

Uncertainties in the jet energy calibration are estimated by shifting the jet energy corrections in simulation up and down by one standard deviation. Depending on p_T and η, the uncertainty in jet energy scale changes by 2–5% [49]. For the signal and backgrounds modeled via simulation, the uncertainty in the measurement is determined from the observed differences in the yields with and without the shift in jet energy corrections. The same technique is used to calculate the uncertainties from the jet energy resolution, which are found to be less than 1% [49]. The b tagging efficiency in the simulation is corrected using scale factors determined from data [50, 65]. These are estimated separately for correctly and incorrectly identified jets, and each results in an uncertainty of about 1–4%, depending on N_b.

To estimate the theoretical uncertainties from the choice of μ_R and μ_F, each of these parameters is varied independently up and down by a factor of 2, ignoring the case, in which one parameter is scaled up while the other is scaled down. The envelope of the acceptance variations is taken as the systematic uncertainty in each search bin and is found to be smaller than 4%. The different sets in the NNPDF3.0 PDF [18] are used to estimate the corresponding uncertainty in the acceptance for the differential cross section measurement, which is typically less than 1%. The uncertainty associated with the choice of PDFs for the anomalous coupling and SMEFT interpretations is estimated by using several PDFs and assigning the maximum differences as the quoted uncertainty, following the PDF4LHC prescription with the MSTW2008 68% CL NNLO, CT10 NNLO, and NNPDF2.3 5f FFN PDF sets (as described in Ref. [28] and references therein, as well as Refs. [66–68]). In the parton shower simulation, the uncertainty from the choice of μ_F is estimated by varying the scale of initial- and final-state radiation up by factors of 2 and $\sqrt{2}$ and down by factors of 0.5 and $1/\sqrt{2}$, respectively, as suggested in Ref. [22]. The default configuration in PYTHIA includes a model of color reconnection based on multiple parton interactions (MPI) with early resonance decays switched off. To estimate the uncertainty from this choice of model, the analysis is repeated with three other color reconnection models within PYTHIA: the MPI-based scheme with early resonance decays switched on, a gluon-move scheme [69], and a QCD-inspired scheme [70]. The total uncertainty from color reconnection modeling is estimated by taking the maximum deviation from the nominal result and amounts to 1.5%.

7 Results

7.1 Inclusive cross section measurement

The observed data, as well as the predicted signal and background yields, are shown in Fig. 3 in various jet and b jet categories, for events with three and four leptons. The signal cross section is extracted from these categories using the statistical procedure detailed in Refs. [71–74]. The observed yields and background estimates in each analysis category, and the systematic uncertainties are used to construct a binned likelihood function $L(r, \theta)$ as a product of Poisson probabilities of all bins. As described in Section 6, the bins of the two data-taking periods are kept separate, and the correlation pattern of the uncertainty as specified in Table 2. The parameter r is the signal strength modifier, i.e., the ratio between the measured cross section and the central value of the cross section predicted by simulation, and θ represents the full suite of nuisance parameters.

The test statistic is the profile likelihood ratio, $q(r) = -2 \ln L(r, \hat{\theta}_r)/L(\hat{r}, \hat{\theta})$, where $\hat{\theta}_r$ reflects the values of the nuisance parameters that maximize the likelihood function for signal strength r. An asymptotic approximation is used to extract the observed cross section of the signal process and the associated uncertainties [71–74]. The quantities $\hat{r}$ and $\hat{\theta}$ are the values that simultaneously maximize L. The fitting procedure is performed for the inclusive cross section

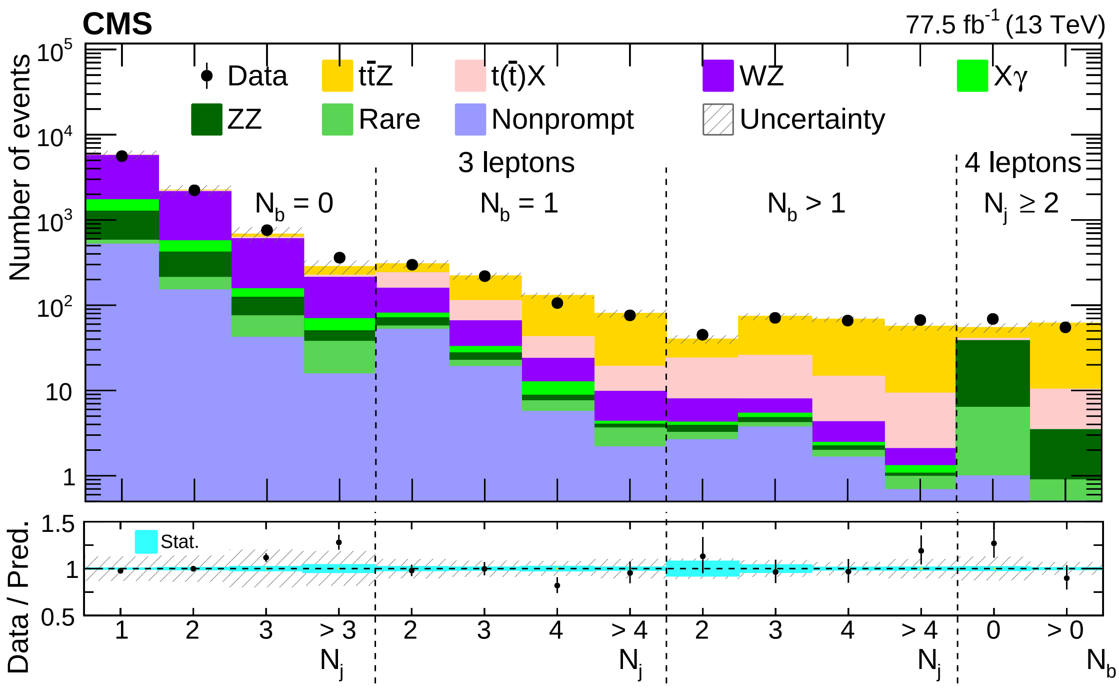

Figure 3: Observed event yields in data for different values of N_j and N_b for events with 3 and 4 leptons, compared with the signal and background yields, as obtained from the fit. The lower panel displays the ratio of the data to the predictions of the signal and background from simulation. The inner and outer bands show the statistical and total uncertainties, respectively.

measurements, and separately for the SMEFT interpretation. The combined cross section of the three- and four-lepton channels within the phase space $70 \leq m(\ell\ell) \leq 110\,\text{GeV}$ for the $\ell\ell$ pair is measured to be

$$\sigma(\text{pp} \to \text{t}\bar{\text{t}}\text{Z}) = 0.95 \pm 0.05\,(\text{stat}) \pm 0.06\,(\text{syst})\,\text{pb},$$

in agreement with the SM prediction of $0.84 \pm 0.10\,\text{pb}$ at NLO and electroweak accuracy [29–31] and $0.86^{+0.07}_{-0.08}\,(\text{scale}) \pm 0.03\,(\text{PDF} + \alpha_S)\,\text{pb}$ including also next-to-next-to-leading-logarithmic (NNLL) corrections [75]. The measured cross sections for the three- and four-lepton channels are given in Table 3.

Table 3: The measured tt̄Z cross section for events with 3 and 4 leptons and the combined measurement.

Lepton requirement	Measured cross section
3ℓ	$0.97 \pm 0.06\,(\text{stat}) \pm 0.06\,(\text{syst})\,\text{pb}$
4ℓ	$0.91 \pm 0.14\,(\text{stat}) \pm 0.08\,(\text{syst})\,\text{pb}$
Total	$0.95 \pm 0.05\,(\text{stat}) \pm 0.06\,(\text{syst})\,\text{pb}$

The background yields and the systematic uncertainties obtained from the fit are, in general, very close to their initial values. The uncertainties associated with the WZ background are modelled using three separate nuisance parameters as described in Section 5. Events in the $N_b = 0$ categories provide a relatively pure WZ control region, which helps constraining two of these uncertainties: the overall normalization uncertainty and the uncertainty in the WZ yields with high jet multiplicity. These uncertainties get constrained, respectively, by 30 and 70% relative to their input values. The third uncertainty controls the WZ production with heavy-flavour jets populating the regions with $N_b \geq 1$, and is not substantially constrained in the fit.

The individual contributions to the total systematic uncertainty in the measured cross section are listed in the fourth column of Table 2. The largest contribution comes from the imperfect knowledge of the lepton selection efficiencies in the signal acceptance. The uncertainties in parton shower modeling and $\mathrm{t}(\bar{\mathrm{t}})\mathrm{X}$ and WZ background yields also form a large fraction of the total uncertainty. With respect to the earlier measurements [3, 4], the statistical (systematic) uncertainty in the inclusive cross section is reduced by about 35 (40)%. The improvement in the systematic uncertainty is primarily the result of a better lepton selection procedure and the detailed studies of its performance in simulation, and an improved estimation of the trigger and b tagging efficiencies in simulation. The reported result is the first experimental measurement that is more precise than the most precise theoretical calculations for $\mathrm{t\bar{t}Z}$ production at NLO in QCD.

A signal-enriched subset of events is selected by requiring $N_\mathrm{b} \geq 1$ and $N_\mathrm{j} \geq 3\,(2)$ for the three (four)-lepton channels. The signal purity is about 65% for these events. Figure 4 shows several kinematic distributions for these signal-enriched events. The sum of the signal and background predictions is found to describe the data within uncertainties. The event yields are listed in Table 4.

Table 4: The observed number of events for three- and four-lepton events in a signal-enriched sample of events, and the predicted yields and total uncertainties from the fit for each process.

Process	$\mu\mu\mu(\mu)$	$\mathrm{e}\mu\mu(\mu)$	$\mathrm{ee}\mu(\mu/\mathrm{e})$	$\mathrm{eee(e)}$	Total
$\mathrm{t\bar{t}Z}$	143 ± 7.1	122 ± 6.1	112 ± 5.5	77 ± 3.9	455 ± 22
$\mathrm{t\bar{t}H}$	4.1 ± 0.5	3.5 ± 0.4	3.3 ± 0.4	2.1 ± 0.3	13 ± 1.6
$\mathrm{t}(\bar{\mathrm{t}})\mathrm{X}$	34 ± 4.2	28 ± 3.4	24 ± 2.9	18 ± 2.3	105 ± 13
WZ	18 ± 4.7	15 ± 4.2	10 ± 2.8	11 ± 3.1	54 ± 15
$\mathrm{X}\gamma$	1.8 ± 1.8	2.1 ± 2.7	0.6 ± 0.6	4.6 ± 1.6	9.0 ± 3.9
ZZ	2.8 ± 0.4	2.7 ± 0.4	2.5 ± 0.3	2.2 ± 0.3	10 ± 1.3
Rare	2.9 ± 1.5	2.1 ± 1.1	1.8 ± 1.0	1.4 ± 0.7	8.3 ± 4.2
Nonprompt	6.9 ± 2.9	11 ± 4.0	6.9 ± 2.9	8.5 ± 3.5	33 ± 13
Total	214 ± 12	187 ± 12	161 ± 9.0	125 ± 8.2	687 ± 40
Observed	192	175	152	141	660

7.2 Differential cross section measurement

The differential cross section is measured as a function of $p_\mathrm{T}(\mathrm{Z})$ and $\cos\theta^*_\mathrm{Z}$. In the simulation, the transverse momentum of the Z boson is taken as the final momentum after any QCD and electroweak radiation. The differential cross section is defined in the same phase space as the inclusive cross section reported above, i.e., in the phase space where the top quark pair is produced in association with two leptons with an invariant mass of $70 \leq m(\ell\ell) \leq 110\,\mathrm{GeV}$, corrected for the detector efficiencies and acceptances, as well as for the branching fraction for the Z boson decay into a pair of muons or electrons.

The measurement of the differential cross section is performed in a signal-enriched sample of events defined by requiring exactly three identified leptons, $N_\mathrm{b} \geq 1$, and $N_\mathrm{j} \geq 3$. Since the data samples under study are statistically limited, a rather coarse binning in $p_\mathrm{T}(\mathrm{Z})$ and $\cos\theta^*_\mathrm{Z}$ is chosen for the differential cross section measurement, with four bins in each distribution.

The cross sections are calculated from the measured event yields corrected for selection and detector effects by subtracting the background and unfolding the resolution effects. The number

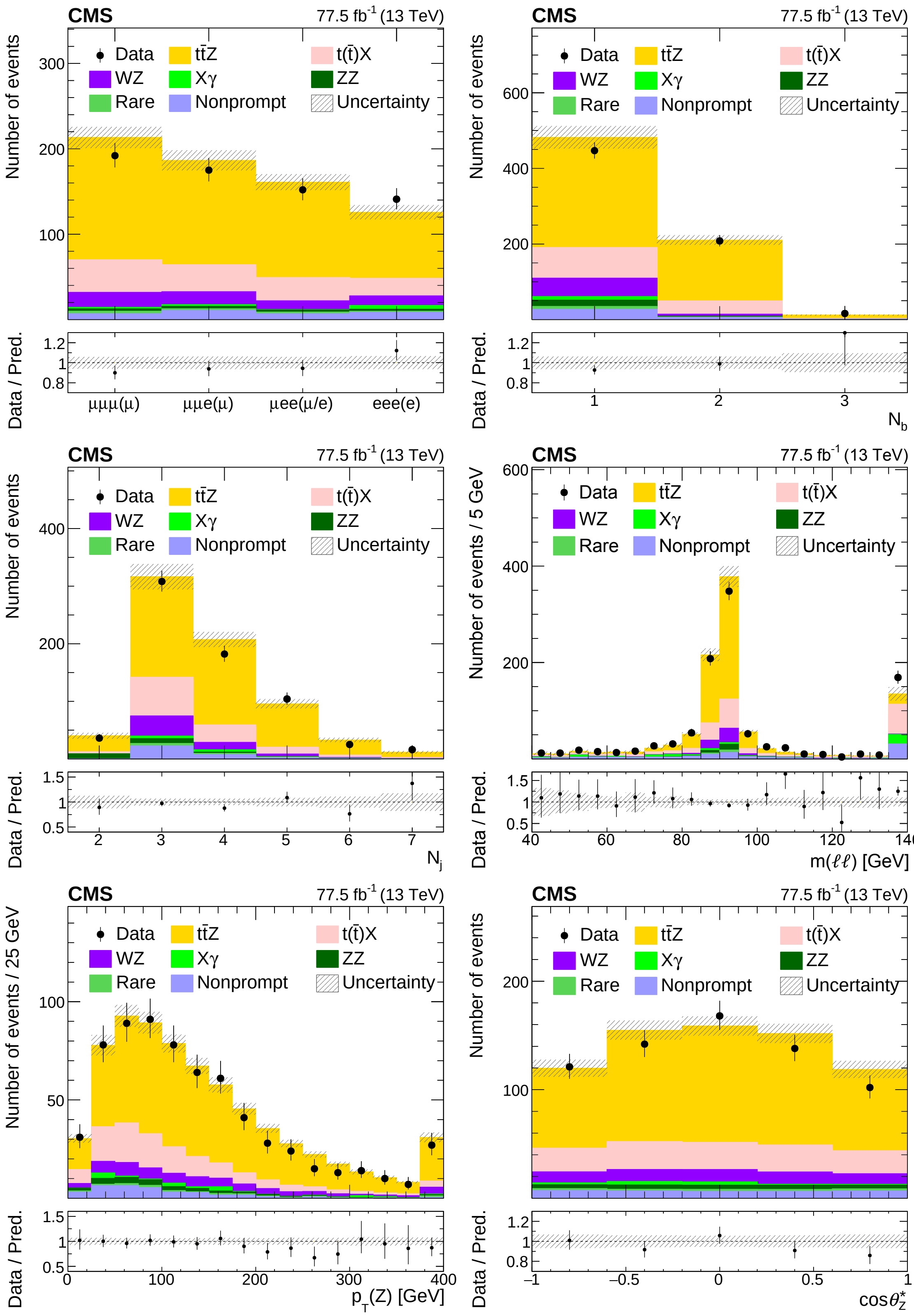

Figure 4: Kinematic distributions from a $t\bar{t}Z$ signal-enriched subset of events for data (points), compared to the contributions of the signal and background yields from the fit (shaded histograms). The distributions include the lepton flavor (upper left), number of b-tagged jets (upper right), jet multiplicity (middle left), dilepton invariant mass $m(\ell\ell)$ (middle right), $p_T(Z)$ (lower left), and $\cos\theta^*_Z$ (lower right). The lower panels in each plot give the ratio of the data to the sum of the signal and background from the fit. The band shows the total uncertainty in the signal and background yields, as obtained from the fit.

of signal events in each bin is determined by subtracting the expected number of background events from the number of events in the data, where the background samples are used without any fit. The $\mathrm{t\bar{t}Z}$ MADGRAPH5_aMC@NLO MC sample is used to construct a response matrix that takes into account both detector response and acceptance corrections. The same corrections, scale factors, and uncertainties as used in the inclusive cross section are applied. Since the resolution of the lepton momenta is good, the fraction of events migrating from one bin to another is extremely small. In all bins, the purity, defined as the fraction of reconstructed events that originate from the same bin, and the stability, defined as the fraction of generated events that are reconstructed in the same bin, are larger than 94%. Under such conditions, matrix inversion without regularization provides an unbiased and stable method to correct for detector response and acceptance [76]. In this analysis, the `TUnfold` package [77] is used to obtain the results for the two measured observables.

For each theoretical uncertainty in the signal sample, such as the choice of μ_R, μ_F, the PDF, and the parton shower, the response matrix is modified and the unfolding procedure is repeated. The uncertainties in the background expectation are accounted for by varying the number of subtracted background events. Experimental uncertainties from the detector response and efficiency, such as the lepton identification, jet energy scale, and b tagging uncertainties, are applied as a function of the reconstructed observable. For the latter uncertainties, the unfolding is performed using the same response matrix as for the nominal result and varying the input data within their uncertainties. This choice is made in order to minimize possible contributions from numerical effects in the matrix inversion.

Figure 5 left and right show, respectively, the measured absolute and normalized differential cross sections as function of $p_{\mathrm{T}}(\mathrm{Z})$ and $\cos\theta^*_{\mathrm{Z}}$, as obtained from the unfolding procedure described above. Also shown is the prediction from the MC generator MADGRAPH5_aMC@NLO with its uncertainty from scale variations, the PDF choice, and the parton shower [29–31], as well as a theory prediction at NLO+NNLL accuracy with its uncertainty from scale variations [75, 78]. Good agreement of the predictions with the measurement is found. The scale variations affect the normalization of the predictions but have negligible impact on their shapes.

7.3 Search for anomalous couplings and effective field theory interpretation

The role of the top quark in many BSM models [5–10] makes its interactions, in particular the electroweak gauge couplings, sensitive probes that can be exploited by interpreting the differential $\mathrm{t\bar{t}Z}$ cross section in models with modified interactions of the top quark and the Z boson. Extending the earlier analysis [3], where the inclusive cross section measurement was used, we consider an anomalous coupling Lagrangian [79]

$$\mathcal{L} = e\bar{u}_{\mathrm{t}}\left[\gamma^\mu\left(C_{1,\mathrm{V}} + \gamma_5 C_{1,\mathrm{A}}\right) + \frac{\mathrm{i}\sigma^{\mu\nu}p_\nu}{m(\mathrm{Z})}\left(C_{2,\mathrm{V}} + \mathrm{i}\gamma_5 C_{2,\mathrm{A}}\right)\right]v_{\bar{\mathrm{t}}}\, Z_\mu,$$

which contains the neutral vector and axial-vector current couplings, $C_{1,\mathrm{V}}$ and $C_{1,\mathrm{A}}$, respectively. The electroweak magnetic and electric dipole interaction couplings are denoted by $C_{1,\mathrm{V}}$ and $C_{1,\mathrm{A}}$, respectively, and the four-momentum of the Z boson is denoted by p_ν. In total, there are four real parameters. The current couplings are exactly predicted by the SM as

$$C_{1,\mathrm{V}}^{\mathrm{SM}} = \frac{I_{3,\mathrm{q}}^{\mathrm{f}} - 2Q_{\mathrm{f}}\sin^2\theta_{\mathrm{W}}}{2\sin\theta_{\mathrm{W}}\cos\theta_{\mathrm{W}}} = 0.2448\,(52),$$

$$C_{1,\mathrm{A}}^{\mathrm{SM}} = \frac{-I_{3,\mathrm{q}}^{\mathrm{f}}}{2\sin\theta_{\mathrm{W}}\cos\theta_{\mathrm{W}}} = -0.6012\,(14),$$

where θ_W is the Weinberg angle, and Q_f and $I_{3,q}^{f}$ label the charge and the third component of the isospin of the SM fermions, respectively [27]. The dipole moments, moreover, are generated only radiatively in the SM. Their small numerical values, which are well below 10^{-3} [5, 80, 81], therefore allow stringent tests of the SM. Beyond $p_T(Z)$, several observables have been considered that are sensitive to anomalous electroweak interactions of the top quark [82]. Among them, $\cos\theta_Z^*$ has a high experimental resolution and provides the best discriminating power when compared to a comprehensive set of alternative choices calculated using the

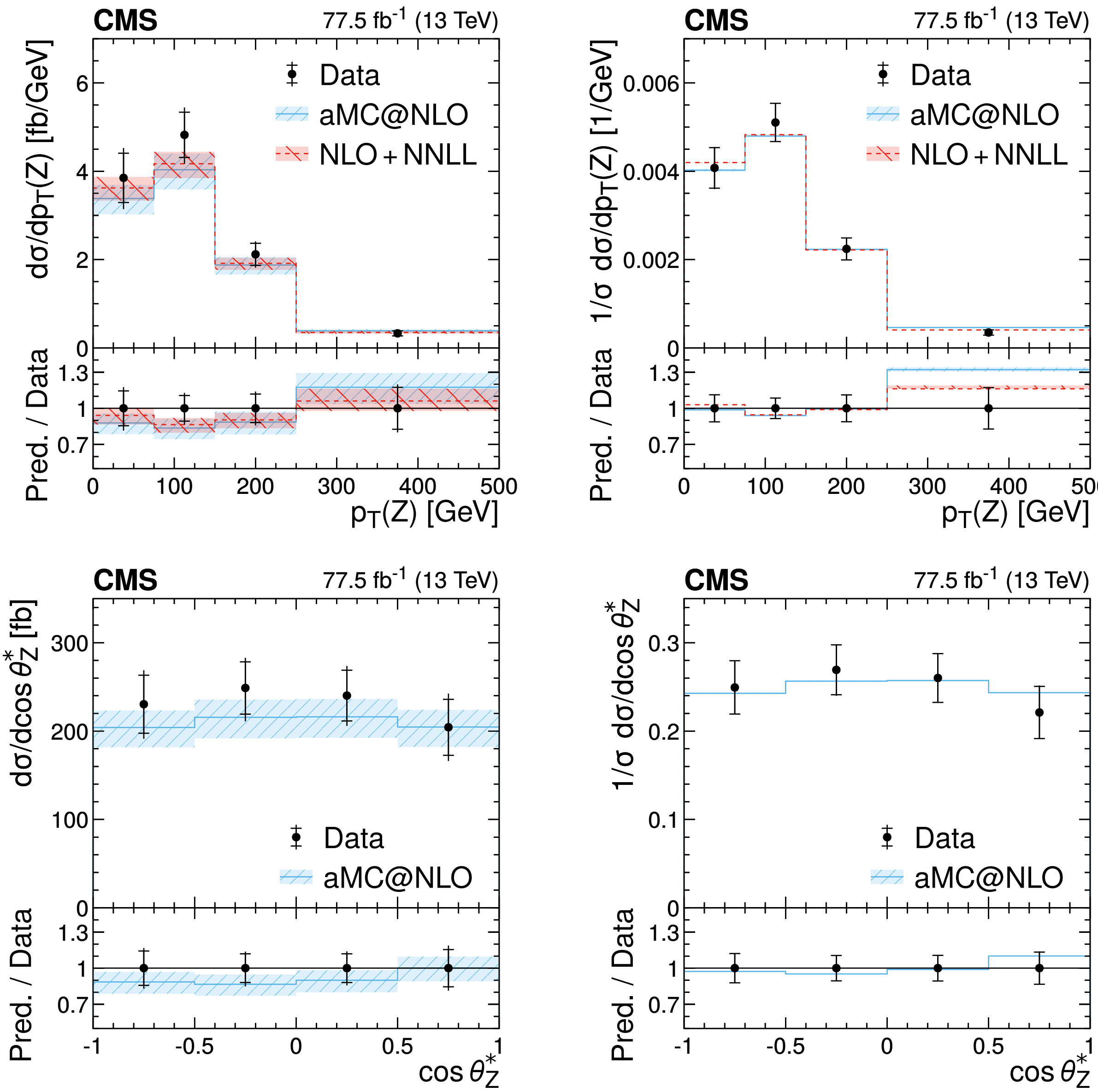

Figure 5: Measured differential $t\bar{t}Z$ production cross sections in the full phase space as a function of the transverse momentum $p_T(Z)$ of the Z boson (upper row) and $\cos\theta_Z^*$, as defined in the text (lower row). Shown are the absolute (left) and normalized (right) cross sections. The data are represented by the points. The inner (outer) vertical lines indicate the statistical (total) uncertainties. The solid histogram shows the prediction from the MADGRAPH5_aMC@NLO MC simulation, and the dashed histogram shows the theory prediction at NLO+NNLL accuracy. The hatched bands indicate the theoretical uncertainties in the predictions, as defined in the text. The lower panels display the ratios of the predictions to the measurement.

reconstructed leptons, jets, and b-tagged jets.

An alternative interpretation is given in the context of SMEFT in the Warsaw basis [12] formed by 59 independent Wilson coefficients of mass dimension 6. Among them, 15 are important for top quark interactions [83], which in general have a large impact on processes other than $\mathrm{t\bar{t}Z}$. Anomalous interactions between the top quark and the gluon (chromomagnetic and chromoelectric dipole moment interactions) are tightly constrained by the $\mathrm{t\bar{t}}$+jets measurement [84]. Similarly, the modification of the Wtb vertex is best constrained by measurements of the W helicity fractions in top quark pair production [85] and in t-channel single top quark production [86]. It is thus appropriate to separately consider the operators that induce anomalous interactions of the top quark with the remaining neutral gauge bosons, the Z boson and the photon. In the parametrization adopted here [13], the relevant Wilson coefficients are c_{tZ}, $c_{\mathrm{tZ}}^{[I]}$, $c_{\phi\mathrm{t}}$, and $c_{\phi\mathrm{Q}}^{-}$. The former two induce electroweak dipole moments, while the latter two induce anomalous neutral-current interactions. These Wilson coefficients, which are combined as

$$
\begin{aligned}
c_{\mathrm{tZ}} &= \mathrm{Re}\left(-\sin\theta_{\mathrm{W}} C_{\mathrm{uB}}^{(33)} + \cos\theta_{\mathrm{W}} C_{\mathrm{uW}}^{(33)}\right) \\
c_{\mathrm{tZ}}^{[I]} &= \mathrm{Im}\left(-\sin\theta_{\mathrm{W}} C_{\mathrm{uB}}^{(33)} + \cos\theta_{\mathrm{W}} C_{\mathrm{uW}}^{(33)}\right) \\
c_{\phi\mathrm{t}} &= C_{\phi\mathrm{t}} = C_{\phi\mathrm{u}}^{(33)} \\
c_{\phi\mathrm{Q}}^{-} &= C_{\phi\mathrm{Q}} = C_{\phi\mathrm{q}}^{1(33)} - C_{\phi\mathrm{q}}^{3(33)},
\end{aligned}
$$

are the main focus of this work. The Wilson coefficients in the Warsaw basis are denoted by $C_{\mathrm{uB}}^{(33)}$, $C_{\mathrm{uW}}^{(33)}$, $C_{\phi\mathrm{u}}^{(33)}$, $C_{\phi\mathrm{q}}^{1(33)}$, and $C_{\phi\mathrm{q}}^{3(33)}$, as defined in Ref. [13]. The constraints $C_{\phi\mathrm{q}}^{3(33)} = 0$ and $C_{\mathrm{uW}}^{(33)} = 0$ ensure a SM Wtb vertex. Wilson coefficients that are not considered in this work are kept at their SM values and the SMEFT expansion parameter is set to $\Lambda = 1\,\mathrm{TeV}$.

Based on the best expected sensitivity, we choose the following signal regions in the three- and four-lepton channels. In the three-lepton channel, there are 12 signal regions defined by the four $p_{\mathrm{T}}(\mathrm{Z})$ thresholds 0, 100, 200, and 400 GeV, and three thresholds on $\cos\theta_{\mathrm{Z}}^{*}$ at -1.0, -0.6, and 0.6. In the four-lepton channel, the predicted event yields are lower, leading to an optimal choice of only three bins defined in terms of $p_{\mathrm{T}}(\mathrm{Z})$ with thresholds at 0, 100, and 200 GeV. The jet multiplicity requirement is relaxed to $N_{\mathrm{j}} \geq 1$. Next, 12 control regions in the three-lepton channel are defined by requiring $N_{\mathrm{b}} = 0$ and $N_{\mathrm{j}} \geq 1$, but otherwise reproducing the three-lepton signal selections. The three-lepton control regions guarantee a pure selection of the main WZ background. In order to also constrain the leading ZZ background of the four-lepton channel, we add three more control regions with $N_{\mathrm{b}} \geq 0$ and $N_{\mathrm{j}} \geq 1$ and require that there be two pairs of opposite-sign same-flavor leptons consistent with the Z boson mass in a window of ± 15 GeV. A summary of the signal and control regions is given in Table 5.

The predictions for signal yields with nonzero values of anomalous couplings or Wilson coefficients are obtained by simulating large LO samples in the respective model on a fine grid in the parameter space, including the SM configuration. Then, the two-dimensional (2D) generator-level distributions of $p_{\mathrm{T}}(\mathrm{Z})$ and $\cos\theta_{\mathrm{Z}}^{*}$ for the BSM and the SM parameter points are used to define the reweighting of the nominal NLO $\mathrm{t\bar{t}Z}$ sample. The result of the reweighting procedure is tested on a coarse grid in BSM parameter space, where BSM samples are produced and reconstructed. The differences between the full event reconstruction and the reweighting procedure are found to be negligible for all distributions considered in this work. The theoretical uncertainties in the predicted BSM yields are scaled accordingly.

From the predicted yields and the uncertainties, we construct a binned likelihood function $L(\theta)$

Table 5: Definition of the signal regions (SRs) and control regions (CRs). For signal regions SR13, SR14, and SR15 and control regions CR13, CR14, and CR15, there is no requirement on $\cos\theta^*_{\mathrm{Z}}$.

N_ℓ	N_{b}	N_{j}	N_{Z}	$p_{\mathrm{T}}(\mathrm{Z})$ (GeV)	$-1 \leq \cos\theta^*_{\mathrm{Z}} < -0.6$	$-0.6 \leq \cos\theta^*_{\mathrm{Z}} < 0.6$	$0.6 \leq \cos\theta^*_{\mathrm{Z}}$
3	≥1	≥3	1	0–100	SR1	SR2	SR3
				100–200	SR4	SR5	SR6
				200–400	SR7	SR8	SR9
				≥400	SR10	SR11	SR12
4	≥1	≥1	1	0–100		SR13	
				100–200		SR14	
				≥200		SR15	
3	0	≥1	1	0–100	CR1	CR2	CR3
				100–200	CR4	CR5	CR6
				200–400	CR7	CR8	CR9
				≥400	CR10	CR11	CR12
4	≥0	≥1	2	0–100		CR13	
				100–200		CR14	
				≥200		CR15	

as a product of Poisson probabilities, where θ labels the set of nuisance parameters. The test statistic is the profile likelihood ratio $q = -2\ln(L(\hat{\theta},\vec{C})/L(\hat{\theta}_{\mathrm{max}}))$ where $\hat{\theta}$ is the set of nuisance parameters maximizing the likelihood function at a BSM point defined by the Wilson coefficients collectively denoted by $\vec{C}$. In the denominator, $\hat{\theta}_{\mathrm{max}}$ maximizes the likelihood function in the BSM parameter plane.

Figure 6 shows the best-fit result in the plane spanned by $c_{\phi\mathrm{t}}$ and $c^{-}_{\phi\mathrm{Q}}$ using the regions in Table 5. Figure 7 displays the log-likelihood scan in the 2D planes spanned by $c_{\phi\mathrm{t}}$ and $c^{-}_{\phi\mathrm{Q}}$, as well as c_{tZ} and $c^{[I]}_{\mathrm{tZ}}$. Consistent with the measurement of the cross section, the SM value is close to the contour in 2D at 95% confidence level (CL) for modified vector and axial-vector current couplings. Models with nonzero electroweak dipole moments predict a harder $p_{\mathrm{T}}(\mathrm{Z})$ spectrum that is not observed in data. A systematic uncertainty from an effect of nonzero Wilson coefficients on the background prediction, in particular of the tZq process amounting to a total of less than 8.5% in the most sensitive bins, was checked to have a negligible impact. The SM prediction is within the 68% confidence interval of the best-fit value of the c_{tZ} and $c^{[I]}_{\mathrm{tZ}}$ coefficients. Figure 8 shows the complementary scan in the 2D plane spanned by the anomalous current interactions $C_{1,\mathrm{V}}$ and $C_{1,\mathrm{A}}$, as well as the anomalous dipole interactions $C_{2,\mathrm{V}}$ and $C_{2,\mathrm{A}}$. In both cases, the SM predictions are consistent with the measurements.

Finally, Figs. 9 and 10 display the one-dimensional (1D) scans, where in each plot, all other coupling parameters are set to their SM values. The corresponding 1D confidence intervals at 68 and 95% CL are listed in Table 6 and are the most stringent direct constraints to date. A comparison of the observed 95% confidence intervals with earlier measurements is shown in Fig. 11, together with direct limits obtained within the SMEFiT framework [87] and by the TopFitter Collaboration [88].

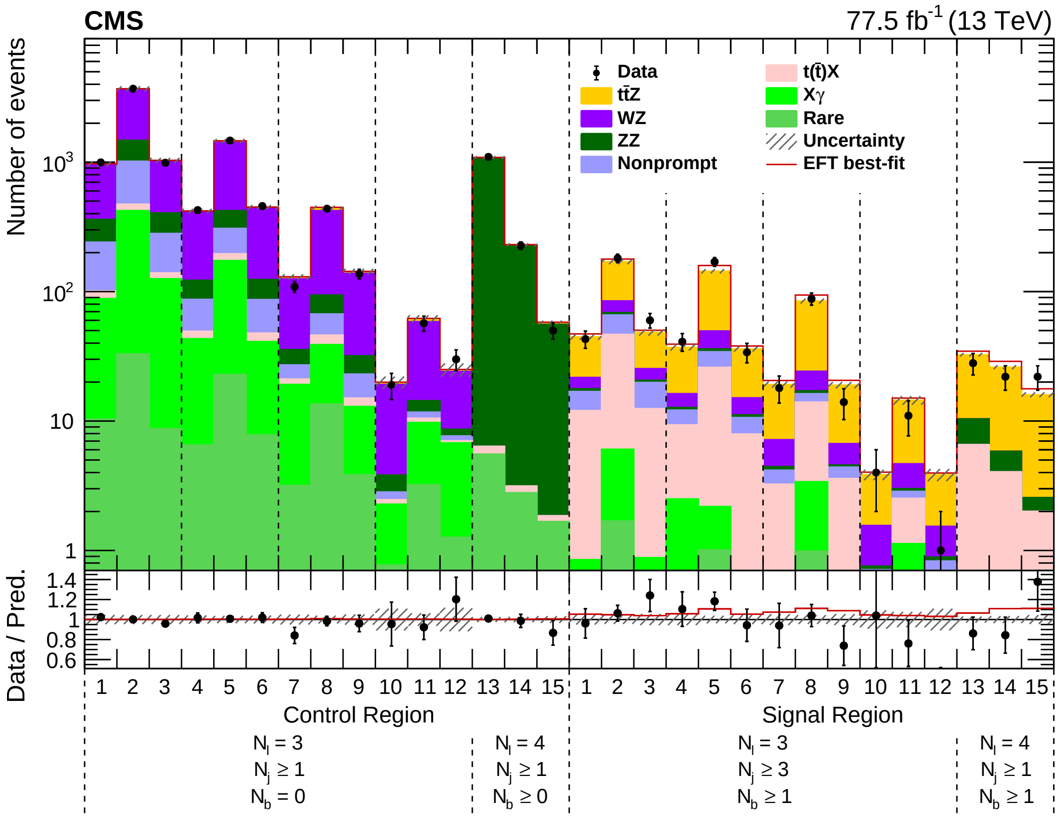

Figure 6: The observed (points) and predicted (shaded histograms) post-fit yields for the combined 2016 and 2017 data sets in the control and signal regions. In the $N_\ell = 3$ control and signal regions (bins 1–12), each of the four $p_T(Z)$ categories is further split into three $\cos\theta^*_Z$ bins. The horizontal bars on the points give the statistical uncertainties in the data. The lower panel displays the ratio of the data to the predictions and the hatched regions show the total uncertainty. The solid line shows the best-fit prediction from the SMEFT fit.

Table 6: Expected and observed 68 and 95% CL intervals from this measurement for the listed Wilson coefficients. The expected and observed 95% CL intervals from a previous CMS measurement [3] and indirect 68% CL constraints from precision electroweak data [90] are shown for comparison.

Coefficient	Expected		Observed		Previous CMS constraints		Indirect constraints
	68% CL	95% CL	68% CL	95% CL	Exp. 95% CL	Obs. 95% CL	68% CL
c_{tZ}/Λ^2	$[-0.7,\ 0.7]$	$[-1.1,\ 1.1]$	$[-0.8,\ 0.5]$	$[-1.1,\ 1.1]$	$[-2.0,\ 2.0]$	$[-2.6,\ 2.6]$	$[-4.7,\ 0.2]$
$c^{[I]}_{tZ}/\Lambda^2$	$[-0.7,\ 0.7]$	$[-1.1,\ 1.1]$	$[-0.8,\ 1.0]$	$[-1.2,\ 1.2]$	—	—	—
$c_{\phi t}/\Lambda^2$	$[-1.6,\ 1.4]$	$[-3.4,\ 2.8]$	$[1.7,\ 4.2]$	$[0.3,\ 5.4]$	$[-20.2,\ 4.0]$	$[-22.2,\ -13.0]$ $[-3.2,\ 6.0]$	$[-0.1,\ 3.7]$
$c^{-}_{\phi Q}/\Lambda^2$	$[-1.1,\ 1.1]$	$[-2.1,\ 2.2]$	$[-3.0,\ -1.0]$	$[-4.0,\ 0.0]$	—	—	$[-4.7,\ 0.7]$

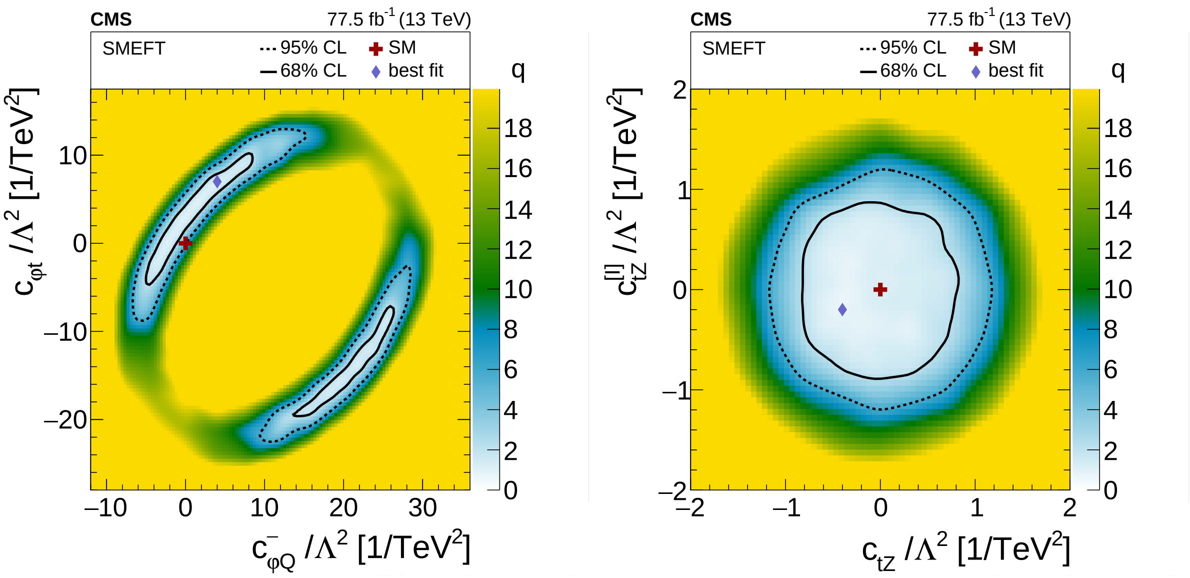

Figure 7: Results of scans in two 2D planes for the SMEFT interpretation. The shading quantified by the gray scale on the right reflects the negative log-likelihood ratio q with respect to the best-fit value, designated by the diamond. The solid and dashed lines indicate the 68 and 95% CL contours from the fit, respectively. The cross shows the SM prediction.

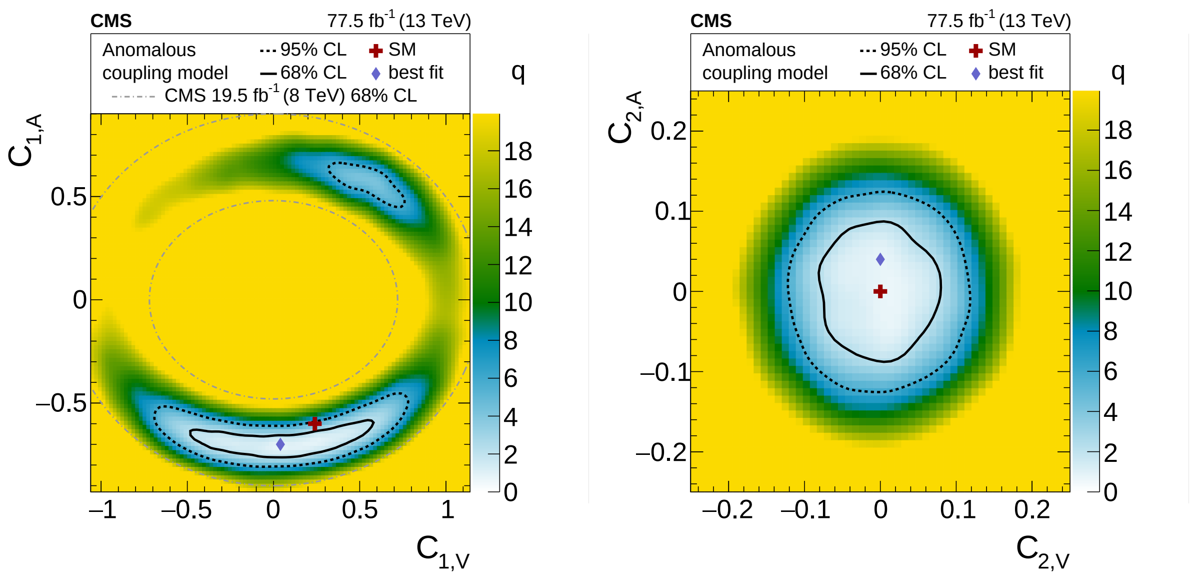

Figure 8: Results of scans in the axial-vector and vector current coupling plane (left) and the electroweak dipole moment plane (right). The shading quantified by the gray scale on the right of each plot reflects the log-likelihood ratio q with respect to the best-fit value, designated by the diamond. The solid and dashed lines indicate the 68 and 95% CL contours from the fit, respectively. The cross shows the SM prediction. The area between the dot-dashed ellipses in the axial-vector and vector current coupling plane corresponds to the observed 68% CL area from the previous CMS result [89].

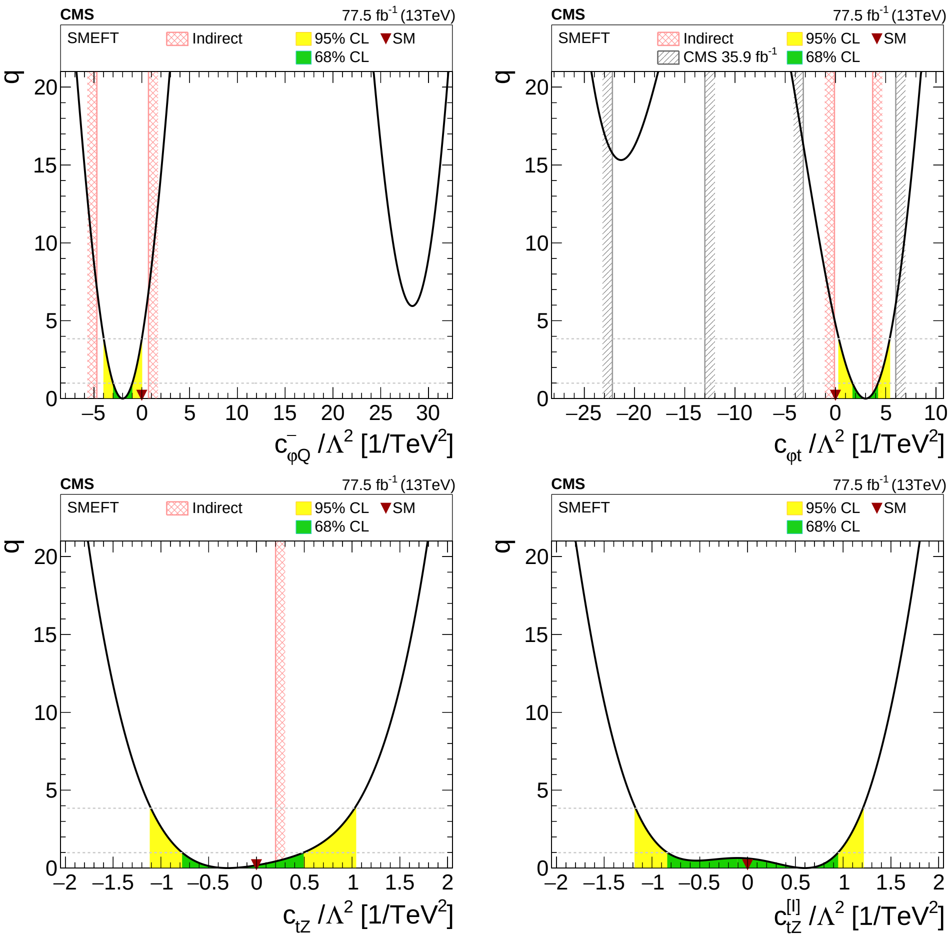

Figure 9: 1D scans of two Wilson coefficients, with the value of the other Wilson coefficients set to zero. The shaded areas correspond to the 68 and 95% CL intervals around the best fit value, respectively. The downward triangle indicates the SM value. Previously excluded regions at 95% CL [3] (if available) are indicated by the hatched band. Indirect constraints from Ref. [90] are shown as a cross-hatched band.

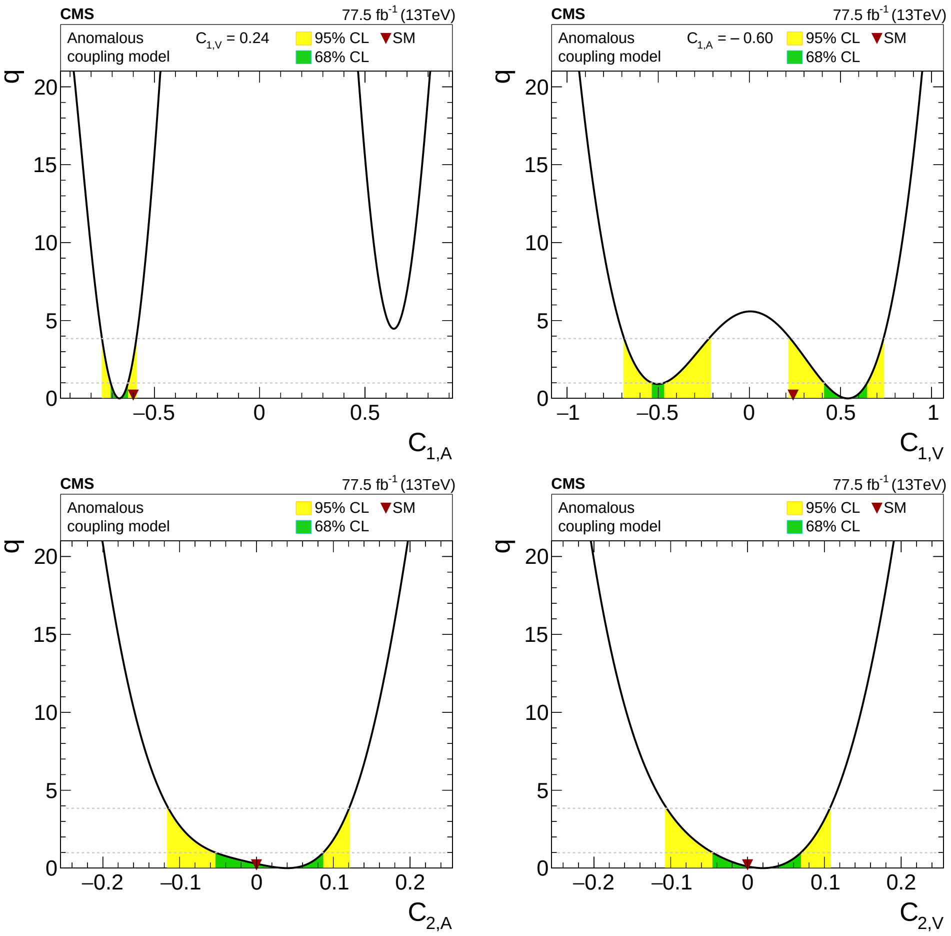

Figure 10: Log-likelihood ratios for 1D scans of anomalous couplings. For the scan of $C_{1,A}$ (upper left), $C_{1,V}$ was set to the SM value of 0.24, and for the scan of $C_{1,V}$ (upper right), $C_{1,A}$ was set to the SM value of -0.60. For the scans of $C_{2,A}$ (lower left) and $C_{2,V}$ (lower right), which correspond to the top quark electric and magnetic dipole moments, respectively, both $C_{1,V}$ and $C_{1,A}$ are set to the SM values. The shaded areas correspond to the 68 and 95% CL intervals around the best-fit value, respectively. The downward triangle indicates the SM value.

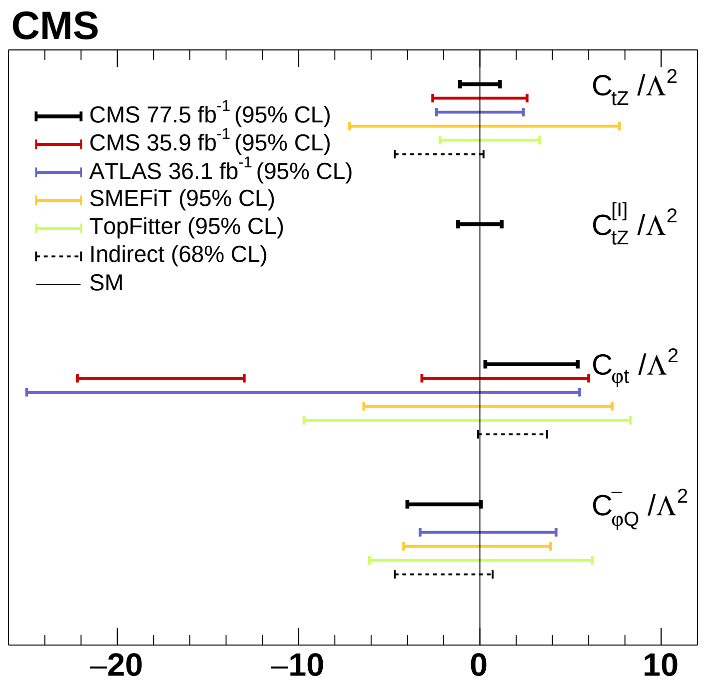

Figure 11: The observed 95% CL intervals for the Wilson coefficients from this measurement, the previous CMS result based on the inclusive $\mathrm{t\bar{t}Z}$ cross section measurement [3], and the most recent ATLAS result [4]. The direct limits within the SMEFiT framework [87] and from the TopFitter Collaboration [88], and the 68% CL indirect limits from electroweak data are also shown [90]. The vertical line displays the SM prediction.

8 Summary

A measurement of top quark pair production in association with a Z boson using a data sample of proton-proton collisions at $\sqrt{s} = 13\,\mathrm{TeV}$, corresponding to an integrated luminosity of $77.5\,\mathrm{fb}^{-1}$, collected with the CMS detector at the LHC has been presented. The analysis was performed in the three- and four-lepton final states using analysis categories defined with jet and b jet multiplicities. Data samples enriched in background processes were used to validate predictions, as well as to constrain their uncertainties. The larger data set and reduced systematic uncertainties such as those associated with the lepton identification, helped to substantially improve the precision on the measured cross section with respect to previous measurements reported in Refs. [3, 4]. The measured inclusive cross section $\sigma(\mathrm{t\bar{t}Z}) = 0.95 \pm 0.05\,(\mathrm{stat}) \pm 0.06\,(\mathrm{syst})\,\mathrm{pb}$ is in good agreement with the standard model prediction of $0.84 \pm 0.10\,\mathrm{pb}$ [29–31]. This is the most precise measurement of the $\mathrm{t\bar{t}Z}$ cross section to date, and the first measurement with a precision competing with current theoretical calculations.

Absolute and normalized differential cross sections for the transverse momentum of the Z boson and for $\cos\theta_Z^*$, the angle between the direction of the Z boson and the direction of the negatively charged lepton in the rest frame of the Z boson, are measured for the first time. The standard model predictions at next-to-leading order are found to be in good agreement with the measured differential cross sections. The measurement is also interpreted in terms of anomalous interactions of the t quark with the Z boson. Confidence intervals for the anomalous vector and the axial-vector current couplings and the dipole moment interactions are presented. Constraints on the Wilson coefficients in the standard model effective field theory are also presented.

Acknowledgments

We congratulate our colleagues in the CERN accelerator departments for the excellent performance of the LHC and thank the technical and administrative staffs at CERN and at other CMS institutes for their contributions to the success of the CMS effort. In addition, we gratefully acknowledge the computing centers and personnel of the Worldwide LHC Computing Grid for delivering so effectively the computing infrastructure essential to our analyses. Finally, we acknowledge the enduring support for the construction and operation of the LHC and the CMS detector provided by the following funding agencies: BMBWF and FWF (Austria); FNRS and FWO (Belgium); CNPq, CAPES, FAPERJ, FAPERGS, and FAPESP (Brazil); MES (Bulgaria); CERN; CAS, MoST, and NSFC (China); COLCIENCIAS (Colombia); MSES and CSF (Croatia); RPF (Cyprus); SENESCYT (Ecuador); MoER, ERC IUT, PUT and ERDF (Estonia); Academy of Finland, MEC, and HIP (Finland); CEA and CNRS/IN2P3 (France); BMBF, DFG, and HGF (Germany); GSRT (Greece); NKFIA (Hungary); DAE and DST (India); IPM (Iran); SFI (Ireland); INFN (Italy); MSIP and NRF (Republic of Korea); MES (Latvia); LAS (Lithuania); MOE and UM (Malaysia); BUAP, CINVESTAV, CONACYT, LNS, SEP, and UASLP-FAI (Mexico); MOS (Montenegro); MBIE (New Zealand); PAEC (Pakistan); MSHE and NSC (Poland); FCT (Portugal); JINR (Dubna); MON, RosAtom, RAS, RFBR, and NRC KI (Russia); MESTD (Serbia); SEIDI, CPAN, PCTI, and FEDER (Spain); MOSTR (Sri Lanka); Swiss Funding Agencies (Switzerland); MST (Taipei); ThEPCenter, IPST, STAR, and NSTDA (Thailand); TUBITAK and TAEK (Turkey); NASU and SFFR (Ukraine); STFC (United Kingdom); DOE and NSF (USA).

Individuals have received support from the Marie-Curie program and the European Research Council and Horizon 2020 Grant, contract Nos. 675440, 752730, and 765710 (European Union); the Leventis Foundation; the A.P. Sloan Foundation; the Alexander von Humboldt Foundation; the Belgian Federal Science Policy Office; the Fonds pour la Formation à la Recherche dans l'Industrie et dans l'Agriculture (FRIA-Belgium); the Agentschap voor Innovatie door Wetenschap en Technologie (IWT-Belgium); the F.R.S.-FNRS and FWO (Belgium) under the "Excellence of Science – EOS" – be.h project n. 30820817; the Beijing Municipal Science & Technology Commission, No. Z181100004218003; the Ministry of Education, Youth and Sports (MEYS) of the Czech Republic; the Lendület ("Momentum") Program and the János Bolyai Research Scholarship of the Hungarian Academy of Sciences, the New National Excellence Program ÚNKP, the NKFIA research grants 123842, 123959, 124845, 124850, 125105, 128713, 128786, and 129058 (Hungary); the Council of Science and Industrial Research, India; the HOMING PLUS program of the Foundation for Polish Science, cofinanced from European Union, Regional Development Fund, the Mobility Plus program of the Ministry of Science and Higher Education, the National Science Center (Poland), contracts Harmonia 2014/14/M/ST2/00428, Opus 2014/13/B/ST2/02543, 2014/15/B/ST2/03998, and 2015/19/B/ST2/02861, Sonata-bis 2012/07/E/ST2/01406; the National Priorities Research Program by Qatar National Research Fund; the Ministry of Science and Education, grant no. 3.2989.2017 (Russia); the Programa Estatal de Fomento de la Investigación Científica y Técnica de Excelencia María de Maeztu, grant MDM-2015-0509 and the Programa Severo Ochoa del Principado de Asturias; the Thalis and Aristeia programs cofinanced by EU-ESF and the Greek NSRF; the Rachadapisek Sompot Fund for Postdoctoral Fellowship, Chulalongkorn University and the Chulalongkorn Academic into Its 2nd Century Project Advancement Project (Thailand); the Welch Foundation, contract C-1845; and the Weston Havens Foundation (USA).

References

[1] O. Bessidskaia Bylund et al., "Probing top quark neutral couplings in the standard model effective field theory at NLO in QCD", *JHEP* **05** (2016) 052, doi:10.1007/JHEP05(2016)052, arXiv:1601.08193.

[2] C. Englert, R. Kogler, H. Schulz, and M. Spannowsky, "Higgs coupling measurements at the LHC", *Eur. Phys. J. C* **76** (2016) 393, doi:10.1140/epjc/s10052-016-4227-1, arXiv:1511.05170.

[3] CMS Collaboration, "Measurement of the cross section for top quark pair production in association with a W or Z boson in proton-proton collisions at $\sqrt{s} = 13$ TeV", *JHEP* **08** (2018) 011, doi:10.1007/JHEP08(2018)011, arXiv:1711.02547.

[4] ATLAS Collaboration, "Measurement of the $\mathrm{t\bar{t}Z}$ and $\mathrm{t\bar{t}W}$ cross sections in proton-proton collisions at $\sqrt{s} = 13$ TeV with the ATLAS detector", *Phys. Rev. D* **99** (2019) 072009, doi:10.1103/PhysRevD.99.072009, arXiv:1901.03584.

[5] W. Hollik et al., "Top dipole form-factors and loop induced CP violation in supersymmetry", *Nucl. Phys. B* **551** (1999) 3, doi:10.1016/S0550-3213(99)00201-1, arXiv:hep-ph/9812298. [Erratum: doi:10.1016/S0550-3213(99)00396-X].

[6] K. Agashe, G. Perez, and A. Soni, "Collider signals of top quark flavor violation from a warped extra dimension", *Phys. Rev. D* **75** (2007) 015002, doi:10.1103/PhysRevD.75.015002, arXiv:hep-ph/0606293.

[7] A. L. Kagan, G. Perez, T. Volansky, and J. Zupan, "General minimal flavor violation", *Phys. Rev. D* **80** (2009) 076002, doi:10.1103/PhysRevD.80.076002, arXiv:0903.1794.

[8] T. Ibrahim and P. Nath, "Top quark electric dipole moment in a minimal supersymmetric standard model extension with vectorlike multiplets", *Phys. Rev. D* **82** (2010) 055001, doi:10.1103/PhysRevD.82.055001, arXiv:1007.0432.

[9] T. Ibrahim and P. Nath, "Chromoelectric dipole moment of the top quark in models with vectorlike multiplets", *Phys. Rev. D* **84** (2011) 015003, doi:10.1103/PhysRevD.84.015003, arXiv:1104.3851.

[10] C. Grojean, O. Matsedonskyi, and G. Panico, "Light top partners and precision physics", *JHEP* **10** (2013) 160, doi:10.1007/JHEP10(2013)160, arXiv:1306.4655.

[11] J. A. Aguilar-Saavedra, "A minimal set of top anomalous couplings", *Nucl. Phys. B* **812** (2009) 181, doi:10.1016/j.nuclphysb.2008.12.012, arXiv:0811.3842.

[12] B. Grzadkowski, M. Iskrzynski, M. Misiak, and J. Rosiek, "Dimension-six terms in the standard model Lagrangian", *JHEP* **10** (2010) 085, doi:10.1007/JHEP10(2010)085, arXiv:1008.4884.

[13] J. A. Aguilar Saavedra et al., "Interpreting top-quark LHC measurements in the standard-model effective field theory", (2018). arXiv:1802.07237.

[14] CMS Collaboration, "The CMS trigger system", *JINST* **12** (2017) P01020, doi:10.1088/1748-0221/12/01/P01020, arXiv:1609.02366.

[15] CMS Collaboration, “The CMS experiment at the CERN LHC”, *JINST* **3** (2008) S08004, doi:10.1088/1748-0221/3/08/S08004.

[16] J. Alwall et al., “The automated computation of tree-level and next-to-leading order differential cross sections, and their matching to parton shower simulations”, *JHEP* **07** (2014) 079, doi:10.1007/JHEP07(2014)079, arXiv:1405.0301.

[17] S. Alioli, P. Nason, C. Oleari, and E. Re, “A general framework for implementing NLO calculations in shower Monte Carlo programs: the POWHEG BOX”, *JHEP* **06** (2010) 043, doi:10.1007/JHEP06(2010)043, arXiv:1002.2581.

[18] NNPDF Collaboration, “Parton distributions for the LHC Run II”, *JHEP* **04** (2015) 040, doi:10.1007/JHEP04(2015)040, arXiv:1410.8849.

[19] NNPDF Collaboration, “Parton distributions from high-precision collider data”, *Eur. Phys. J. C* **77** (2017) 663, doi:10.1140/epjc/s10052-017-5199-5, arXiv:1706.00428.

[20] T. Sjöstrand, S. Mrenna, and P. Z. Skands, “A brief introduction to PYTHIA 8.1”, *Comput. Phys. Commun.* **178** (2008) 852, doi:10.1016/j.cpc.2008.01.036, arXiv:0710.3820.

[21] T. Sjöstrand et al., “An introduction to PYTHIA 8.2”, *Comput. Phys. Commun.* **191** (2015) 159, doi:10.1016/j.cpc.2015.01.024, arXiv:1410.3012.

[22] P. Skands, S. Carrazza, and J. Rojo, “Tuning PYTHIA 8.1: the Monash 2013 tune”, *Eur. Phys. J. C* **74** (2014) 3024, doi:10.1140/epjc/s10052-014-3024-y, arXiv:1404.5630.

[23] CMS Collaboration, “Event generator tunes obtained from underlying event and multiparton scattering measurements”, *Eur. Phys. J. C* **76** (2016) 155, doi:10.1140/epjc/s10052-016-3988-x, arXiv:1512.00815.

[24] CMS Collaboration, “Extraction and validation of a new set of CMS PYTHIA8 tunes from underlying-event measurements”, *Eur. Phys. J. C* **80** (2020) 4, doi:10.1140/epjc/s10052-019-7499-4, arXiv:1903.12179.

[25] CMS Collaboration, “Investigations of the impact of the parton shower tuning in PYTHIA 8 in the modelling of $\mathrm{t\bar{t}}$ at $\sqrt{s} = 8$ and 13 TeV”, CMS Physics Analysis Summary CMS-PAS-TOP-16-021, 2016.

[26] R. Frederix and S. Frixione, “Merging meets matching in MC@NLO”, *JHEP* **12** (2012) 061, doi:10.1007/JHEP12(2012)061, arXiv:1209.6215.

[27] Particle Data Group, M. Tanabashi et al., “Review of particle physics”, *Phys. Rev. D* **98** (2018) 030001, doi:10.1103/PhysRevD.98.030001.

[28] J. Butterworth et al., “PDF4LHC recommendations for LHC Run II”, *J. Phys. G* **43** (2016) 023001, doi:10.1088/0954-3899/43/2/023001, arXiv:1510.03865.

[29] D. de Florian et al., “Handbook of LHC Higgs cross sections: 4. Deciphering the nature of the Higgs sector”, CERN Report CERN-2017-002-M, 2016. doi:10.23731/CYRM-2017-002, arXiv:1610.07922.

[30] S. Frixione et al., "Electroweak and QCD corrections to top-pair hadroproduction in association with heavy bosons", *JHEP* **06** (2015) 184, doi:10.1007/JHEP06(2015)184, arXiv:1504.03446.

[31] R. Frederix et al., "The automation of next-to-leading order electroweak calculations", *JHEP* **07** (2018) 185, doi:10.1007/JHEP07(2018)185, arXiv:1804.10017.

[32] F. Caola, K. Melnikov, R. Röntsch, and L. Tancredi, "QCD corrections to ZZ production in gluon fusion at the LHC", *Phys. Rev. D* **92** (2015) 094028, doi:10.1103/PhysRevD.92.094028, arXiv:1509.06734.

[33] J. M. Campbell and R. K. Ellis, "MCFM for the Tevatron and the LHC", *Nucl. Phys. Proc. Suppl.* **205-206** (2010) 10, doi:10.1016/j.nuclphysbps.2010.08.011, arXiv:1007.3492.

[34] S. Bolognesi et al., "Spin and parity of a single-produced resonance at the LHC", *Phys. Rev. D* **86** (2012) 095031, doi:10.1103/PhysRevD.86.095031, arXiv:1208.4018.

[35] F. Cascioli et al., "ZZ production at hadron colliders in NNLO QCD", *Phys. Lett. B* **735** (2014) 311, doi:10.1016/j.physletb.2014.06.056, arXiv:1405.2219.

[36] T. Melia, P. Nason, R. Rontsch, and G. Zanderighi, "W^+W^-, WZ and ZZ production in the POWHEG BOX", *JHEP* **11** (2011) 078, doi:10.1007/JHEP11(2011)078, arXiv:1107.5051.

[37] P. Nason and G. Zanderighi, "W^+W^- , WZ and ZZ production in the POWHEG-BOX-V2", *Eur. Phys. J. C* **74** (2014) 2702, doi:10.1140/epjc/s10052-013-2702-5, arXiv:1311.1365.

[38] G. Luisoni, P. Nason, C. Oleari, and F. Tramontano, "$HW^\pm$/HZ + 0 and 1 jet at NLO with the POWHEG BOX interfaced to GoSam and their merging within MiNLO", *JHEP* **10** (2013) 083, doi:10.1007/JHEP10(2013)083, arXiv:1306.2542.

[39] H. B. Hartanto, B. Jager, L. Reina, and D. Wackeroth, "Higgs boson production in association with top quarks in the POWHEG BOX", *Phys. Rev. D* **91** (2015) 094003, doi:10.1103/PhysRevD.91.094003, arXiv:1501.04498.

[40] M. Czakon and A. Mitov, "Top++: A program for the calculation of the top-pair cross section at hadron colliders", *Comput. Phys. Commun.* **185** (2014) 2930, doi:10.1016/j.cpc.2014.06.021, arXiv:1112.5675.

[41] GEANT4 Collaboration, "GEANT4—a simulation toolkit", *Nucl. Instrum. Meth. A* **506** (2003) 250, doi:10.1016/S0168-9002(03)01368-8.

[42] CMS Collaboration, "Particle-flow reconstruction and global event description with the CMS detector", *JINST* **12** (2017) P10003, doi:10.1088/1748-0221/12/10/P10003, arXiv:1706.04965.

[43] CMS Collaboration, "Performance of electron reconstruction and selection with the CMS detector in proton-proton collisions at $\sqrt{s} = 8\,\mathrm{TeV}$", *JINST* **10** (2015) P06005, doi:10.1088/1748-0221/10/06/P06005, arXiv:1502.02701.

[44] CMS Collaboration, "Performance of CMS muon reconstruction in pp collision events at $\sqrt{s} = 7\,\mathrm{TeV}$", *JINST* **7** (2012) P10002, doi:10.1088/1748-0221/7/10/P10002, arXiv:1206.4071.

[45] M. Cacciari, G. P. Salam, and G. Soyez, "The anti-k_T jet clustering algorithm", *JHEP* **04** (2008) 063, doi:10.1088/1126-6708/2008/04/063, arXiv:0802.1189.

[46] M. Cacciari, G. P. Salam, and G. Soyez, "FastJet user manual", *Eur. Phys. J. C* **72** (2012) 1896, doi:10.1140/epjc/s10052-012-1896-2, arXiv:1111.6097.

[47] CMS Collaboration, "Pileup removal algorithms", CMS Physics Analysis Summary CMS-PAS-JME-14-001, 2014.

[48] CMS Collaboration, "Determination of jet energy calibration and transverse momentum resolution in CMS", *JINST* **6** (2011) P11002, doi:10.1088/1748-0221/6/11/P11002, arXiv:1107.4277.

[49] CMS Collaboration, "Jet energy scale and resolution in the CMS experiment in pp collisions at 8 TeV", *JINST* **12** (2017) P02014, doi:10.1088/1748-0221/12/02/P02014, arXiv:1607.03663.

[50] CMS Collaboration, "Identification of heavy-flavour jets with the CMS detector in pp collisions at 13 TeV", *JINST* **13** (2018) P05011, doi:10.1088/1748-0221/13/05/P05011, arXiv:1712.07158.

[51] CMS Collaboration, "Observation of $t\bar{t}H$ production", *Phys. Rev. Lett.* **120** (2018) 231801, doi:10.1103/PhysRevLett.120.231801, arXiv:1804.02610.

[52] H. Voss, A. Höcker, J. Stelzer, and F. Tegenfeldt, "TMVA, the toolkit for multivariate data analysis with ROOT", in *XIth International Workshop on Advanced Computing and Analysis Techniques in Physics Research (ACAT)*, p. 40. 2007. [PoS(ACAT)040]. doi:10.22323/1.050.0040.

[53] CMS Collaboration, "Search for supersymmetry in pp collisions at $\sqrt{s} = 13$ TeV in the single-lepton final state using the sum of masses of large-radius jets", *JHEP* **08** (2016) 122, doi:10.1007/JHEP08(2016)122, arXiv:1605.04608.

[54] J. Campbell, R. K. Ellis, and R. Röntsch, "Single top production in association with a Z boson at the LHC", *Phys. Rev. D* **87** (2013) 114006, doi:10.1103/PhysRevD.87.114006, arXiv:1302.3856.

[55] CMS Collaboration, "Observation of single top quark production in association with a Z boson in proton-proton collisions at $\sqrt{s} = 13$ TeV", *Phys. Rev. Lett.* **122** (2019) 132003, doi:10.1103/PhysRevLett.122.132003, arXiv:1812.05900.

[56] CMS Collaboration, "Measurement of differential cross sections for Z boson pair production in association with jets at $\sqrt{s} = 8$ and 13 TeV", *Phys. Lett. B* **789** (2019) 19, doi:10.1016/j.physletb.2018.11.007, arXiv:1806.11073.

[57] CMS Collaboration, "Measurements of the pp $\to$ WZ inclusive and differential production cross section and constraints on charged anomalous triple gauge couplings at $\sqrt{s} = 13$ TeV", *JHEP* **04** (2019) 122, doi:10.1007/JHEP04(2019)122, arXiv:1901.03428.

[58] D. T. Nhung, L. D. Ninh, and M. M. Weber, "NLO corrections to WWZ production at the LHC", *JHEP* **12** (2013) 096, doi:10.1007/JHEP12(2013)096, arXiv:1307.7403.

[59] CMS Collaboration, "Measurement of the Zγ production cross section in pp collisions at 8 TeV and search for anomalous triple gauge boson couplings", *JHEP* **04** (2015) 164, doi:10.1007/JHEP04(2015)164, arXiv:1502.05664.

[60] CMS Collaboration, "Measurement of the cross section for electroweak production of Zγ in association with two jets and constraints on anomalous quartic gauge couplings in proton-proton collisions at $\sqrt{s} = 8$ TeV", *Phys. Lett. B* **770** (2017) 380, doi:10.1016/j.physletb.2017.04.071, arXiv:1702.03025.

[61] CMS Collaboration, "CMS luminosity measurements for the 2016 data taking period", CMS Physics Analysis Summary CMS-PAS-LUM-17-001, 2017.

[62] CMS Collaboration, "CMS luminosity measurement for the 2017 data-taking period at $\sqrt{s} = 13$ TeV", CMS Physics Analysis Summary CMS-PAS-LUM-17-004, 2018.

[63] CMS Collaboration, "Measurement of the inelastic proton-proton cross section at $\sqrt{s} = 13$ TeV", *JHEP* **07** (2018) 161, doi:10.1007/JHEP07(2018)161, arXiv:1802.02613.

[64] ATLAS Collaboration, "Measurement of the inelastic proton-proton cross section at $\sqrt{s} = 13$ TeV with the ATLAS detector at the LHC", *Phys. Rev. Lett.* **117** (2016) 182002, doi:10.1103/PhysRevLett.117.182002, arXiv:1606.02625.

[65] CMS Collaboration, "Identification of b-quark jets with the CMS experiment", *JINST* **8** (2013) P04013, doi:10.1088/1748-0221/8/04/P04013, arXiv:1211.4462.

[66] R. D. Ball et al., "Parton distributions with LHC data", *Nucl. Phys. B* **867** (2013) 244, doi:10.1016/j.nuclphysb.2012.10.003, arXiv:1207.1303.

[67] A. D. Martin, W. J. Stirling, R. S. Thorne, and G. Watt, "Uncertainties on α_S in global PDF analyses and implications for predicted hadronic cross sections", *Eur. Phys. J. C* **64** (2009) 653, doi:10.1140/epjc/s10052-009-1164-2, arXiv:0905.3531.

[68] J. Gao et al., "CT10 next-to-next-to-leading order global analysis of QCD", *Phys. Rev. D* **89** (2014) 033009, doi:10.1103/PhysRevD.89.033009, arXiv:1302.6246.

[69] S. Argyropoulos and T. Sjöstrand, "Effects of color reconnection on $\mathrm{t\bar{t}}$ final states at the LHC", *JHEP* **11** (2014) 043, doi:10.1007/JHEP11(2014)043, arXiv:1407.6653.

[70] J. R. Christiansen and P. Z. Skands, "String formation beyond leading colour", *JHEP* **08** (2015) 003, doi:10.1007/JHEP08(2015)003, arXiv:1505.01681.

[71] T. Junk, "Confidence level computation for combining searches with small statistics", *Nucl. Instrum. Meth. A* **434** (1999) 435, doi:10.1016/S0168-9002(99)00498-2, arXiv:hep-ex/9902006.

[72] A. L. Read, "Presentation of search results: The $\mathrm{CL_s}$ technique", *J. Phys. G* **28** (2002) 2693, doi:10.1088/0954-3899/28/10/313.

[73] ATLAS and CMS Collaborations and LHC Higgs Combination Group, "Procedure for the LHC Higgs boson search combination in summer 2011", ATL-PHYS-PUB-2011-011, CMS-NOTE-2011-005, 2011.

[74] G. Cowan, K. Cranmer, E. Gross, and O. Vitells, "Asymptotic formulae for likelihood-based tests of new physics", *Eur. Phys. J. C* **71** (2011) 1554, doi:10.1140/epjc/s10052-011-1554-0, arXiv:1007.1727. [Erratum: doi:10.1140/epjc/s10052-013-2501-z].

[75] A. Kulesza et al., "Associated production of a top quark pair with a heavy electroweak gauge boson at NLO+NNLL accuracy", *Eur. Phys. J. C* **79** (2019) 249, doi:10.1140/epjc/s10052-019-6746-z, arXiv:1812.08622.

[76] G. Cowan, "Statistical data analysis". Clarendon Press, Oxford, 1998.

[77] S. Schmitt, "TUnfold, an algorithm for correcting migration effects in high energy physics", *JINST* **7** (2012) T10003, doi:10.1088/1748-0221/7/10/T10003, arXiv:1205.6201.

[78] A. Kulesza et al., "Associated top-pair production with a heavy boson production through NLO+NNLL accuracy at the LHC", in *54th Rencontres de Moriond on QCD and High Energy Interactions (Moriond QCD 2019), La Thuile, Italy, March 23-30, 2019*. 2019. arXiv:1905.07815.

[79] R. Röntsch and M. Schulze, "Constraining couplings of top quarks to the Z boson in $t\bar{t}$+Z production at the LHC", *JHEP* **07** (2014) 091, doi:10.1007/JHEP07(2014)091, arXiv:1404.1005. [Erratum: doi:10.1007/JHEP09(2015)132].

[80] J. Bernabeu, D. Comelli, L. Lavoura, and J. P. Silva, "Weak magnetic dipole moments in two-Higgs-doublet models", *Phys. Rev. D* **53** (1996) 5222, doi:10.1103/PhysRevD.53.5222, arXiv:hep-ph/9509416.

[81] A. Czarnecki and B. Krause, "On the dipole moments of fermions at two loops", *Acta Phys. Polon. B* **28** (1997) 829, arXiv:hep-ph/9611299.

[82] M. Schulze and Y. Soreq, "Pinning down electroweak dipole operators of the top quark", *Eur. Phys. J. C* **76** (2016) 466, doi:10.1140/epjc/s10052-016-4263-x, arXiv:1603.08911.

[83] C. Zhang and S. Willenbrock, "Effective-field-theory approach to top-quark production and decay", *Phys. Rev. D* **83** (2011) 034006, doi:10.1103/PhysRevD.83.034006, arXiv:1008.3869.

[84] CMS Collaboration, "Measurements of $t\bar{t}$ differential cross sections in proton-proton collisions at $\sqrt{s} = 13$ TeV using events containing two leptons", *JHEP* **02** (2019) 149, doi:10.1007/JHEP02(2019)149, arXiv:1811.06625.

[85] CMS Collaboration, "Measurement of the W boson helicity fractions in the decays of top quark pairs to lepton+jets final states produced in pp collisions at $\sqrt{s} = 8$ TeV", *Phys. Lett. B* **762** (2016) 512, doi:10.1016/j.physletb.2016.10.007, arXiv:1605.09047.

[86] J. A. Aguilar-Saavedra and J. Bernabeu, "W polarisation beyond helicity fractions in top quark decays", *Nucl. Phys. B* **840** (2010) 349, doi:10.1016/j.nuclphysb.2010.07.012, arXiv:1005.5382.

[87] N. P. Hartland et al., "A Monte Carlo global analysis of the standard model effective field theory: the top quark sector", *JHEP* **04** (2019) 100, doi:10.1007/JHEP04(2019)100, arXiv:1901.05965.

[88] A. Buckley et al., "Constraining top quark effective theory in the LHC Run II era", *JHEP* **04** (2016) 015, doi:10.1007/JHEP04(2016)015, arXiv:1512.03360.

[89] CMS Collaboration, "Observation of top quark pairs produced in association with a vector boson in pp collisions at $\sqrt{s} = 8$ TeV", *JHEP* **01** (2016) 096, doi:10.1007/JHEP01(2016)096, arXiv:1510.01131.

[90] C. Zhang, N. Greiner, and S. Willenbrock, "Constraints on nonstandard top quark couplings", *Phys. Rev. D* **86** (2012) 014024, doi:10.1103/PhysRevD.86.014024, arXiv:1201.6670.

A The CMS Collaboration

Yerevan Physics Institute, Yerevan, Armenia
A.M. Sirunyan[†], A. Tumasyan

Institut für Hochenergiephysik, Wien, Austria
W. Adam, F. Ambrogi, T. Bergauer, J. Brandstetter, M. Dragicevic, J. Erö, A. Escalante Del Valle, M. Flechl, R. Frühwirth[1], M. Jeitler[1], N. Krammer, I. Krätschmer, D. Liko, T. Madlener, I. Mikulec, N. Rad, J. Schieck[1], R. Schöfbeck, M. Spanring, D. Spitzbart, W. Waltenberger, C.-E. Wulz[1], M. Zarucki

Institute for Nuclear Problems, Minsk, Belarus
V. Drugakov, V. Mossolov, J. Suarez Gonzalez

Universiteit Antwerpen, Antwerpen, Belgium
M.R. Darwish, E.A. De Wolf, D. Di Croce, X. Janssen, J. Lauwers, A. Lelek, M. Pieters, H. Rejeb Sfar, H. Van Haevermaet, P. Van Mechelen, S. Van Putte, N. Van Remortel

Vrije Universiteit Brussel, Brussel, Belgium
F. Blekman, E.S. Bols, S.S. Chhibra, J. D'Hondt, J. De Clercq, D. Lontkovskyi, S. Lowette, I. Marchesini, S. Moortgat, L. Moreels, Q. Python, K. Skovpen, S. Tavernier, W. Van Doninck, P. Van Mulders, I. Van Parijs

Université Libre de Bruxelles, Bruxelles, Belgium
D. Beghin, B. Bilin, H. Brun, B. Clerbaux, G. De Lentdecker, H. Delannoy, B. Dorney, L. Favart, A. Grebenyuk, A.K. Kalsi, J. Luetic, A. Popov, N. Postiau, E. Starling, L. Thomas, C. Vander Velde, P. Vanlaer, D. Vannerom, Q. Wang

Ghent University, Ghent, Belgium
T. Cornelis, D. Dobur, I. Khvastunov[2], C. Roskas, D. Trocino, M. Tytgat, W. Verbeke, B. Vermassen, M. Vit, N. Zaganidis

Université Catholique de Louvain, Louvain-la-Neuve, Belgium
O. Bondu, G. Bruno, C. Caputo, P. David, C. Delaere, M. Delcourt, A. Giammanco, V. Lemaitre, A. Magitteri, J. Prisciandaro, A. Saggio, M. Vidal Marono, P. Vischia, J. Zobec

Centro Brasileiro de Pesquisas Fisicas, Rio de Janeiro, Brazil
F.L. Alves, G.A. Alves, G. Correia Silva, C. Hensel, A. Moraes, P. Rebello Teles

Universidade do Estado do Rio de Janeiro, Rio de Janeiro, Brazil
E. Belchior Batista Das Chagas, W. Carvalho, J. Chinellato[3], E. Coelho, E.M. Da Costa, G.G. Da Silveira[4], D. De Jesus Damiao, C. De Oliveira Martins, S. Fonseca De Souza, L.M. Huertas Guativa, H. Malbouisson, J. Martins[5], D. Matos Figueiredo, M. Medina Jaime[6], M. Melo De Almeida, C. Mora Herrera, L. Mundim, H. Nogima, W.L. Prado Da Silva, L.J. Sanchez Rosas, A. Santoro, A. Sznajder, M. Thiel, E.J. Tonelli Manganote[3], F. Torres Da Silva De Araujo, A. Vilela Pereira

Universidade Estadual Paulista [a], Universidade Federal do ABC [b], São Paulo, Brazil
S. Ahuja[a], C.A. Bernardes[a], L. Calligaris[a], T.R. Fernandez Perez Tomei[a], E.M. Gregores[b], D.S. Lemos, P.G. Mercadante[b], S.F. Novaes[a], SandraS. Padula[a]

Institute for Nuclear Research and Nuclear Energy, Bulgarian Academy of Sciences, Sofia, Bulgaria
A. Aleksandrov, G. Antchev, R. Hadjiiska, P. Iaydjiev, A. Marinov, M. Misheva, M. Rodozov, M. Shopova, G. Sultanov

University of Sofia, Sofia, Bulgaria
M. Bonchev, A. Dimitrov, T. Ivanov, L. Litov, B. Pavlov, P. Petkov

Beihang University, Beijing, China
W. Fang[7], X. Gao[7], L. Yuan

Institute of High Energy Physics, Beijing, China
M. Ahmad, G.M. Chen, H.S. Chen, M. Chen, C.H. Jiang, D. Leggat, H. Liao, Z. Liu, S.M. Shaheen[8], A. Spiezia, J. Tao, E. Yazgan, H. Zhang, S. Zhang[8], J. Zhao

State Key Laboratory of Nuclear Physics and Technology, Peking University, Beijing, China
A. Agapitos, Y. Ban, G. Chen, A. Levin, J. Li, L. Li, Q. Li, Y. Mao, S.J. Qian, D. Wang

Tsinghua University, Beijing, China
Z. Hu, Y. Wang

Universidad de Los Andes, Bogota, Colombia
C. Avila, A. Cabrera, L.F. Chaparro Sierra, C. Florez, C.F. González Hernández, M.A. Segura Delgado

Universidad de Antioquia, Medellin, Colombia
J. Mejia Guisao, J.D. Ruiz Alvarez, C.A. Salazar González, N. Vanegas Arbelaez

University of Split, Faculty of Electrical Engineering, Mechanical Engineering and Naval Architecture, Split, Croatia
D. Giljanović, N. Godinovic, D. Lelas, I. Puljak, T. Sculac

University of Split, Faculty of Science, Split, Croatia
Z. Antunovic, M. Kovac

Institute Rudjer Boskovic, Zagreb, Croatia
V. Brigljevic, S. Ceci, D. Ferencek, K. Kadija, B. Mesic, M. Roguljic, A. Starodumov[9], T. Susa

University of Cyprus, Nicosia, Cyprus
M.W. Ather, A. Attikis, E. Erodotou, A. Ioannou, M. Kolosova, S. Konstantinou, G. Mavromanolakis, J. Mousa, C. Nicolaou, F. Ptochos, P.A. Razis, H. Rykaczewski, D. Tsiakkouri

Charles University, Prague, Czech Republic
M. Finger[10], M. Finger Jr.[10], A. Kveton, J. Tomsa

Escuela Politecnica Nacional, Quito, Ecuador
E. Ayala

Universidad San Francisco de Quito, Quito, Ecuador
E. Carrera Jarrin

Academy of Scientific Research and Technology of the Arab Republic of Egypt, Egyptian Network of High Energy Physics, Cairo, Egypt
H. Abdalla[11], A.A. Abdelalim[12,13]

National Institute of Chemical Physics and Biophysics, Tallinn, Estonia
S. Bhowmik, A. Carvalho Antunes De Oliveira, R.K. Dewanjee, K. Ehataht, M. Kadastik, M. Raidal, C. Veelken

Department of Physics, University of Helsinki, Helsinki, Finland
P. Eerola, L. Forthomme, H. Kirschenmann, K. Osterberg, M. Voutilainen

Helsinki Institute of Physics, Helsinki, Finland
F. Garcia, J. Havukainen, J.K. Heikkilä, T. Järvinen, V. Karimäki, R. Kinnunen, T. Lampén, K. Lassila-Perini, S. Laurila, S. Lehti, T. Lindén, P. Luukka, T. Mäenpää, H. Siikonen, E. Tuominen, J. Tuominiemi

Lappeenranta University of Technology, Lappeenranta, Finland
T. Tuuva

IRFU, CEA, Université Paris-Saclay, Gif-sur-Yvette, France
M. Besancon, F. Couderc, M. Dejardin, D. Denegri, B. Fabbro, J.L. Faure, F. Ferri, S. Ganjour, A. Givernaud, P. Gras, G. Hamel de Monchenault, P. Jarry, C. Leloup, E. Locci, J. Malcles, J. Rander, A. Rosowsky, M.Ö. Sahin, A. Savoy-Navarro[14], M. Titov

Laboratoire Leprince-Ringuet, CNRS/IN2P3, Ecole Polytechnique, Institut Polytechnique de Paris
C. Amendola, F. Beaudette, P. Busson, C. Charlot, B. Diab, G. Falmagne, R. Granier de Cassagnac, I. Kucher, A. Lobanov, C. Martin Perez, M. Nguyen, C. Ochando, P. Paganini, J. Rembser, R. Salerno, J.B. Sauvan, Y. Sirois, A. Zabi, A. Zghiche

Université de Strasbourg, CNRS, IPHC UMR 7178, Strasbourg, France
J.-L. Agram[15], J. Andrea, D. Bloch, G. Bourgatte, J.-M. Brom, E.C. Chabert, C. Collard, E. Conte[15], J.-C. Fontaine[15], D. Gelé, U. Goerlach, M. Jansová, A.-C. Le Bihan, N. Tonon, P. Van Hove

Centre de Calcul de l'Institut National de Physique Nucleaire et de Physique des Particules, CNRS/IN2P3, Villeurbanne, France
S. Gadrat

Université de Lyon, Université Claude Bernard Lyon 1, CNRS-IN2P3, Institut de Physique Nucléaire de Lyon, Villeurbanne, France
S. Beauceron, C. Bernet, G. Boudoul, C. Camen, N. Chanon, R. Chierici, D. Contardo, P. Depasse, H. El Mamouni, J. Fay, S. Gascon, M. Gouzevitch, B. Ille, Sa. Jain, F. Lagarde, I.B. Laktineh, H. Lattaud, M. Lethuillier, L. Mirabito, S. Perries, V. Sordini, G. Touquet, M. Vander Donckt, S. Viret

Georgian Technical University, Tbilisi, Georgia
T. Toriashvili[16]

Tbilisi State University, Tbilisi, Georgia
Z. Tsamalaidze[10]

RWTH Aachen University, I. Physikalisches Institut, Aachen, Germany
C. Autermann, L. Feld, M.K. Kiesel, K. Klein, M. Lipinski, D. Meuser, A. Pauls, M. Preuten, M.P. Rauch, C. Schomakers, J. Schulz, M. Teroerde, B. Wittmer

RWTH Aachen University, III. Physikalisches Institut A, Aachen, Germany
A. Albert, M. Erdmann, S. Erdweg, T. Esch, B. Fischer, R. Fischer, S. Ghosh, T. Hebbeker, K. Hoepfner, H. Keller, L. Mastrolorenzo, M. Merschmeyer, A. Meyer, P. Millet, G. Mocellin, S. Mondal, S. Mukherjee, D. Noll, A. Novak, T. Pook, A. Pozdnyakov, T. Quast, M. Radziej, Y. Rath, H. Reithler, M. Rieger, J. Roemer, A. Schmidt, S.C. Schuler, A. Sharma, S. Thüer, S. Wiedenbeck

RWTH Aachen University, III. Physikalisches Institut B, Aachen, Germany
G. Flügge, W. Haj Ahmad[17], O. Hlushchenko, T. Kress, T. Müller, A. Nehrkorn, A. Nowack, C. Pistone, O. Pooth, D. Roy, H. Sert, A. Stahl[18]

Deutsches Elektronen-Synchrotron, Hamburg, Germany
M. Aldaya Martin, P. Asmuss, I. Babounikau, H. Bakhshiansohi, K. Beernaert, O. Behnke, U. Behrens, A. Bermúdez Martínez, D. Bertsche, A.A. Bin Anuar, K. Borras[19], V. Botta, A. Campbell, A. Cardini, P. Connor, S. Consuegra Rodríguez, C. Contreras-Campana, V. Danilov, A. De Wit, M.M. Defranchis, C. Diez Pardos, D. Domínguez Damiani, G. Eckerlin, D. Eckstein, T. Eichhorn, A. Elwood, E. Eren, E. Gallo[20], A. Geiser, J.M. Grados Luyando, A. Grohsjean, M. Guthoff, M. Haranko, A. Harb, A. Jafari, N.Z. Jomhari, H. Jung, A. Kasem[19], M. Kasemann, H. Kaveh, J. Keaveney, C. Kleinwort, J. Knolle, D. Krücker, W. Lange, T. Lenz, J. Leonard, J. Lidrych, K. Lipka, W. Lohmann[21], R. Mankel, I.-A. Melzer-Pellmann, A.B. Meyer, M. Meyer, M. Missiroli, G. Mittag, J. Mnich, A. Mussgiller, V. Myronenko, D. Pérez Adán, S.K. Pflitsch, D. Pitzl, A. Raspereza, A. Saibel, M. Savitskyi, V. Scheurer, P. Schütze, C. Schwanenberger, R. Shevchenko, A. Singh, H. Tholen, O. Turkot, A. Vagnerini, M. Van De Klundert, G.P. Van Onsem, R. Walsh, Y. Wen, K. Wichmann, C. Wissing, O. Zenaiev, R. Zlebcik

University of Hamburg, Hamburg, Germany
R. Aggleton, S. Bein, L. Benato, A. Benecke, V. Blobel, T. Dreyer, A. Ebrahimi, A. Fröhlich, C. Garbers, E. Garutti, D. Gonzalez, P. Gunnellini, J. Haller, A. Hinzmann, A. Karavdina, G. Kasieczka, R. Klanner, R. Kogler, N. Kovalchuk, S. Kurz, V. Kutzner, J. Lange, T. Lange, A. Malara, D. Marconi, J. Multhaup, M. Niedziela, C.E.N. Niemeyer, D. Nowatschin, A. Perieanu, A. Reimers, O. Rieger, C. Scharf, P. Schleper, S. Schumann, J. Schwandt, J. Sonneveld, H. Stadie, G. Steinbrück, F.M. Stober, M. Stöver, B. Vormwald, I. Zoi

Karlsruher Institut fuer Technologie, Karlsruhe, Germany
M. Akbiyik, C. Barth, M. Baselga, S. Baur, T. Berger, E. Butz, R. Caspart, T. Chwalek, W. De Boer, A. Dierlamm, K. El Morabit, N. Faltermann, M. Giffels, P. Goldenzweig, A. Gottmann, M.A. Harrendorf, F. Hartmann[18], U. Husemann, S. Kudella, S. Mitra, M.U. Mozer, Th. Müller, M. Musich, A. Nürnberg, G. Quast, K. Rabbertz, M. Schröder, I. Shvetsov, H.J. Simonis, R. Ulrich, M. Weber, C. Wöhrmann, R. Wolf

Institute of Nuclear and Particle Physics (INPP), NCSR Demokritos, Aghia Paraskevi, Greece
G. Anagnostou, P. Asenov, G. Daskalakis, T. Geralis, A. Kyriakis, D. Loukas, G. Paspalaki

National and Kapodistrian University of Athens, Athens, Greece
M. Diamantopoulou, G. Karathanasis, P. Kontaxakis, A. Panagiotou, I. Papavergou, N. Saoulidou, A. Stakia, K. Theofilatos, K. Vellidis

National Technical University of Athens, Athens, Greece
G. Bakas, K. Kousouris, I. Papakrivopoulos, G. Tsipolitis

University of Ioánnina, Ioánnina, Greece
I. Evangelou, C. Foudas, P. Gianneios, P. Katsoulis, P. Kokkas, S. Mallios, K. Manitara, N. Manthos, I. Papadopoulos, J. Strologas, F.A. Triantis, D. Tsitsonis

MTA-ELTE Lendület CMS Particle and Nuclear Physics Group, Eötvös Loránd University, Budapest, Hungary
M. Bartók[22], M. Csanad, P. Major, K. Mandal, A. Mehta, M.I. Nagy, G. Pasztor, O. Surányi, G.I. Veres

Wigner Research Centre for Physics, Budapest, Hungary
G. Bencze, C. Hajdu, D. Horvath[23], F. Sikler, T.. Vámi, V. Veszpremi, G. Vesztergombi[†]

Institute of Nuclear Research ATOMKI, Debrecen, Hungary
N. Beni, S. Czellar, J. Karancsi[22], A. Makovec, J. Molnar, Z. Szillasi

Institute of Physics, University of Debrecen, Debrecen, Hungary
P. Raics, D. Teyssier, Z.L. Trocsanyi, B. Ujvari

Eszterhazy Karoly University, Karoly Robert Campus, Gyongyos, Hungary
T. Csorgo, W.J. Metzger, F. Nemes, T. Novak

Indian Institute of Science (IISc), Bangalore, India
S. Choudhury, J.R. Komaragiri, P.C. Tiwari

National Institute of Science Education and Research, HBNI, Bhubaneswar, India
S. Bahinipati[25], C. Kar, G. Kole, P. Mal, V.K. Muraleedharan Nair Bindhu, A. Nayak[26], D.K. Sahoo[25], S.K. Swain

Panjab University, Chandigarh, India
S. Bansal, S.B. Beri, V. Bhatnagar, S. Chauhan, R. Chawla, N. Dhingra, R. Gupta, A. Kaur, M. Kaur, S. Kaur, P. Kumari, M. Lohan, M. Meena, K. Sandeep, S. Sharma, J.B. Singh, A.K. Virdi

University of Delhi, Delhi, India
A. Bhardwaj, B.C. Choudhary, R.B. Garg, M. Gola, S. Keshri, Ashok Kumar, S. Malhotra, M. Naimuddin, P. Priyanka, K. Ranjan, Aashaq Shah, R. Sharma

Saha Institute of Nuclear Physics, HBNI, Kolkata, India
R. Bhardwaj[27], M. Bharti[27], R. Bhattacharya, S. Bhattacharya, U. Bhawandeep[27], D. Bhowmik, S. Dey, S. Dutta, S. Ghosh, M. Maity[28], K. Mondal, S. Nandan, A. Purohit, P.K. Rout, A. Roy, G. Saha, S. Sarkar, T. Sarkar[28], M. Sharan, B. Singh[27], S. Thakur[27]

Indian Institute of Technology Madras, Madras, India
P.K. Behera, P. Kalbhor, A. Muhammad, P.R. Pujahari, A. Sharma, A.K. Sikdar

Bhabha Atomic Research Centre, Mumbai, India
R. Chudasama, D. Dutta, V. Jha, V. Kumar, D.K. Mishra, P.K. Netrakanti, L.M. Pant, P. Shukla

Tata Institute of Fundamental Research-A, Mumbai, India
T. Aziz, M.A. Bhat, S. Dugad, G.B. Mohanty, N. Sur, RavindraKumar Verma

Tata Institute of Fundamental Research-B, Mumbai, India
S. Banerjee, S. Bhattacharya, S. Chatterjee, P. Das, M. Guchait, S. Karmakar, S. Kumar, G. Majumder, K. Mazumdar, N. Sahoo, S. Sawant

Indian Institute of Science Education and Research (IISER), Pune, India
S. Chauhan, S. Dube, V. Hegde, A. Kapoor, K. Kothekar, S. Pandey, A. Rane, A. Rastogi, S. Sharma

Institute for Research in Fundamental Sciences (IPM), Tehran, Iran
S. Chenarani[29], E. Eskandari Tadavani, S.M. Etesami[29], M. Khakzad, M. Mohammadi Najafabadi, M. Naseri, F. Rezaei Hosseinabadi

University College Dublin, Dublin, Ireland
M. Felcini, M. Grunewald

INFN Sezione di Bari [a], Università di Bari [b], Politecnico di Bari [c], Bari, Italy
M. Abbrescia[a,b], C. Calabria[a,b], A. Colaleo[a], D. Creanza[a,c], L. Cristella[a,b], N. De Filippis[a,c], M. De Palma[a,b], A. Di Florio[a,b], L. Fiore[a], A. Gelmi[a,b], G. Iaselli[a,c], M. Ince[a,b], S. Lezki[a,b],

G. Maggi[a,c], M. Maggi[a], G. Miniello[a,b], S. My[a,b], S. Nuzzo[a,b], A. Pompili[a,b], G. Pugliese[a,c], R. Radogna[a], A. Ranieri[a], G. Selvaggi[a,b], L. Silvestris[a], R. Venditti[a], P. Verwilligen[a]

INFN Sezione di Bologna [a], Università di Bologna [b], Bologna, Italy
G. Abbiendi[a], C. Battilana[a,b], D. Bonacorsi[a,b], L. Borgonovi[a,b], S. Braibant-Giacomelli[a,b], R. Campanini[a,b], P. Capiluppi[a,b], A. Castro[a,b], F.R. Cavallo[a], C. Ciocca[a], G. Codispoti[a,b], M. Cuffiani[a,b], G.M. Dallavalle[a], F. Fabbri[a], A. Fanfani[a,b], E. Fontanesi, P. Giacomelli[a], C. Grandi[a], L. Guiducci[a,b], F. Iemmi[a,b], S. Lo Meo[a,30], S. Marcellini[a], G. Masetti[a], F.L. Navarria[a,b], A. Perrotta[a], F. Primavera[a,b], A.M. Rossi[a,b], T. Rovelli[a,b], G.P. Siroli[a,b], N. Tosi[a]

INFN Sezione di Catania [a], Università di Catania [b], Catania, Italy
S. Albergo[a,b,31], S. Costa[a,b], A. Di Mattia[a], R. Potenza[a,b], A. Tricomi[a,b,31], C. Tuve[a,b]

INFN Sezione di Firenze [a], Università di Firenze [b], Firenze, Italy
G. Barbagli[a], R. Ceccarelli, K. Chatterjee[a,b], V. Ciulli[a,b], C. Civinini[a], R. D'Alessandro[a,b], E. Focardi[a,b], G. Latino, P. Lenzi[a,b], M. Meschini[a], S. Paoletti[a], G. Sguazzoni[a], D. Strom[a], L. Viliani[a]

INFN Laboratori Nazionali di Frascati, Frascati, Italy
L. Benussi, S. Bianco, D. Piccolo

INFN Sezione di Genova [a], Università di Genova [b], Genova, Italy
M. Bozzo[a,b], F. Ferro[a], R. Mulargia[a,b], E. Robutti[a], S. Tosi[a,b]

INFN Sezione di Milano-Bicocca [a], Università di Milano-Bicocca [b], Milano, Italy
A. Benaglia[a], A. Beschi[a,b], F. Brivio[a,b], V. Ciriolo[a,b,18], S. Di Guida[a,b,18], M.E. Dinardo[a,b], P. Dini[a], S. Fiorendi[a,b], S. Gennai[a], A. Ghezzi[a,b], P. Govoni[a,b], L. Guzzi[a,b], M. Malberti[a], S. Malvezzi[a], D. Menasce[a], F. Monti[a,b], L. Moroni[a], G. Ortona[a,b], M. Paganoni[a,b], D. Pedrini[a], S. Ragazzi[a,b], T. Tabarelli de Fatis[a,b], D. Zuolo[a,b]

INFN Sezione di Napoli [a], Università di Napoli 'Federico II' [b], Napoli, Italy, Università della Basilicata [c], Potenza, Italy, Università G. Marconi [d], Roma, Italy
S. Buontempo[a], N. Cavallo[a,c], A. De Iorio[a,b], A. Di Crescenzo[a,b], F. Fabozzi[a,c], F. Fienga[a], G. Galati[a], A.O.M. Iorio[a,b], L. Lista[a,b], S. Meola[a,d,18], P. Paolucci[a,18], B. Rossi[a], C. Sciacca[a,b], E. Voevodina[a,b]

INFN Sezione di Padova [a], Università di Padova [b], Padova, Italy, Università di Trento [c], Trento, Italy
P. Azzi[a], N. Bacchetta[a], A. Boletti[a,b], A. Bragagnolo, R. Carlin[a,b], P. Checchia[a], P. De Castro Manzano[a], T. Dorigo[a], U. Dosselli[a], F. Gasparini[a,b], U. Gasparini[a,b], A. Gozzelino[a], S.Y. Hoh, P. Lujan, M. Margoni[a,b], A.T. Meneguzzo[a,b], J. Pazzini[a,b], N. Pozzobon[a,b], M. Presilla[b], P. Ronchese[a,b], R. Rossin[a,b], F. Simonetto[a,b], A. Tiko, M. Tosi[a,b], M. Zanetti[a,b], P. Zotto[a,b], G. Zumerle[a,b]

INFN Sezione di Pavia [a], Università di Pavia [b], Pavia, Italy
A. Braghieri[a], P. Montagna[a,b], S.P. Ratti[a,b], V. Re[a], M. Ressegotti[a,b], C. Riccardi[a,b], P. Salvini[a], I. Vai[a,b], P. Vitulo[a,b]

INFN Sezione di Perugia [a], Università di Perugia [b], Perugia, Italy
M. Biasini[a,b], G.M. Bilei[a], C. Cecchi[a,b], D. Ciangottini[a,b], L. Fanò[a,b], P. Lariccia[a,b], R. Leonardi[a,b], E. Manoni[a], G. Mantovani[a,b], V. Mariani[a,b], M. Menichelli[a], A. Rossi[a,b], A. Santocchia[a,b], D. Spiga[a]

INFN Sezione di Pisa [a], Università di Pisa [b], Scuola Normale Superiore di Pisa [c], Pisa, Italy
K. Androsov[a], P. Azzurri[a], G. Bagliesi[a], V. Bertacchi[a,c], L. Bianchini[a], T. Boccali[a],

R. Castaldi[a], M.A. Ciocci[a,b], R. Dell'Orso[a], G. Fedi[a], L. Giannini[a,c], A. Giassi[a], M.T. Grippo[a], F. Ligabue[a,c], E. Manca[a,c], G. Mandorli[a,c], A. Messineo[a,b], F. Palla[a], A. Rizzi[a,b], G. Rolandi[32], S. Roy Chowdhury, A. Scribano[a], P. Spagnolo[a], R. Tenchini[a], G. Tonelli[a,b], N. Turini, A. Venturi[a], P.G. Verdini[a]

INFN Sezione di Roma [a], Sapienza Università di Roma [b], Rome, Italy
F. Cavallari[a], M. Cipriani[a,b], D. Del Re[a,b], E. Di Marco[a,b], M. Diemoz[a], E. Longo[a,b], B. Marzocchi[a,b], P. Meridiani[a], G. Organtini[a,b], F. Pandolfi[a], R. Paramatti[a,b], C. Quaranta[a,b], S. Rahatlou[a,b], C. Rovelli[a], F. Santanastasio[a,b], L. Soffi[a,b]

INFN Sezione di Torino [a], Università di Torino [b], Torino, Italy, Università del Piemonte Orientale [c], Novara, Italy
N. Amapane[a,b], R. Arcidiacono[a,c], S. Argiro[a,b], M. Arneodo[a,c], N. Bartosik[a], R. Bellan[a,b], C. Biino[a], A. Cappati[a,b], N. Cartiglia[a], S. Cometti[a], M. Costa[a,b], R. Covarelli[a,b], N. Demaria[a], B. Kiani[a,b], C. Mariotti[a], S. Maselli[a], E. Migliore[a,b], V. Monaco[a,b], E. Monteil[a,b], M. Monteno[a], M.M. Obertino[a,b], L. Pacher[a,b], N. Pastrone[a], M. Pelliccioni[a], G.L. Pinna Angioni[a,b], A. Romero[a,b], M. Ruspa[a,c], R. Sacchi[a,b], R. Salvatico[a,b], V. Sola[a], A. Solano[a,b], D. Soldi[a,b], A. Staiano[a]

INFN Sezione di Trieste [a], Università di Trieste [b], Trieste, Italy
S. Belforte[a], V. Candelise[a,b], M. Casarsa[a], F. Cossutti[a], A. Da Rold[a,b], G. Della Ricca[a,b], F. Vazzoler[a,b], A. Zanetti[a]

Kyungpook National University, Daegu, Korea
B. Kim, D.H. Kim, G.N. Kim, M.S. Kim, J. Lee, S.W. Lee, C.S. Moon, Y.D. Oh, S.I. Pak, S. Sekmen, D.C. Son, Y.C. Yang

Chonnam National University, Institute for Universe and Elementary Particles, Kwangju, Korea
H. Kim, D.H. Moon, G. Oh

Hanyang University, Seoul, Korea
B. Francois, T.J. Kim, J. Park

Korea University, Seoul, Korea
S. Cho, S. Choi, Y. Go, D. Gyun, S. Ha, B. Hong, K. Lee, K.S. Lee, J. Lim, J. Park, S.K. Park, Y. Roh

Kyung Hee University, Department of Physics
J. Goh

Sejong University, Seoul, Korea
H.S. Kim

Seoul National University, Seoul, Korea
J. Almond, J.H. Bhyun, J. Choi, S. Jeon, J. Kim, J.S. Kim, H. Lee, K. Lee, S. Lee, K. Nam, M. Oh, S.B. Oh, B.C. Radburn-Smith, U.K. Yang, H.D. Yoo, I. Yoon, G.B. Yu

University of Seoul, Seoul, Korea
D. Jeon, H. Kim, J.H. Kim, J.S.H. Lee, I.C. Park, I. Watson

Sungkyunkwan University, Suwon, Korea
Y. Choi, C. Hwang, Y. Jeong, J. Lee, Y. Lee, I. Yu

Riga Technical University, Riga, Latvia
V. Veckalns[33]

Vilnius University, Vilnius, Lithuania
V. Dudenas, A. Juodagalvis, J. Vaitkus

National Centre for Particle Physics, Universiti Malaya, Kuala Lumpur, Malaysia
Z.A. Ibrahim, F. Mohamad Idris[34], W.A.T. Wan Abdullah, M.N. Yusli, Z. Zolkapli

Universidad de Sonora (UNISON), Hermosillo, Mexico
J.F. Benitez, A. Castaneda Hernandez, J.A. Murillo Quijada, L. Valencia Palomo

Centro de Investigacion y de Estudios Avanzados del IPN, Mexico City, Mexico
H. Castilla-Valdez, E. De La Cruz-Burelo, I. Heredia-De La Cruz[35], R. Lopez-Fernandez, A. Sanchez-Hernandez

Universidad Iberoamericana, Mexico City, Mexico
S. Carrillo Moreno, C. Oropeza Barrera, M. Ramirez-Garcia, F. Vazquez Valencia

Benemerita Universidad Autonoma de Puebla, Puebla, Mexico
J. Eysermans, I. Pedraza, H.A. Salazar Ibarguen, C. Uribe Estrada

Universidad Autónoma de San Luis Potosí, San Luis Potosí, Mexico
A. Morelos Pineda

University of Montenegro, Podgorica, Montenegro
N. Raicevic

University of Auckland, Auckland, New Zealand
D. Krofcheck

University of Canterbury, Christchurch, New Zealand
S. Bheesette, P.H. Butler

National Centre for Physics, Quaid-I-Azam University, Islamabad, Pakistan
A. Ahmad, M. Ahmad, Q. Hassan, H.R. Hoorani, W.A. Khan, M.A. Shah, M. Shoaib, M. Waqas

AGH University of Science and Technology Faculty of Computer Science, Electronics and Telecommunications, Krakow, Poland
V. Avati, L. Grzanka, M. Malawski

National Centre for Nuclear Research, Swierk, Poland
H. Bialkowska, M. Bluj, B. Boimska, M. Górski, M. Kazana, M. Szleper, P. Zalewski

Institute of Experimental Physics, Faculty of Physics, University of Warsaw, Warsaw, Poland
K. Bunkowski, A. Byszuk[36], K. Doroba, A. Kalinowski, M. Konecki, J. Krolikowski, M. Misiura, M. Olszewski, A. Pyskir, M. Walczak

Laboratório de Instrumentação e Física Experimental de Partículas, Lisboa, Portugal
M. Araujo, P. Bargassa, D. Bastos, A. Di Francesco, P. Faccioli, B. Galinhas, M. Gallinaro, J. Hollar, N. Leonardo, J. Seixas, K. Shchelina, G. Strong, O. Toldaiev, J. Varela

Joint Institute for Nuclear Research, Dubna, Russia
P. Bunin, M. Gavrilenko, I. Golutvin, A. Kamenev, V. Karjavine, I. Kashunin, V. Korenkov, G. Kozlov, A. Lanev, A. Malakhov, V. Matveev[37,38], V.V. Mitsyn, P. Moisenz, V. Palichik, V. Perelygin, S. Shmatov, N. Voytishin, B.S. Yuldashev[39], A. Zarubin, V. Zhiltsov

Petersburg Nuclear Physics Institute, Gatchina (St. Petersburg), Russia
L. Chtchipounov, V. Golovtsov, Y. Ivanov, V. Kim[40], E. Kuznetsova[41], P. Levchenko, V. Murzin, V. Oreshkin, I. Smirnov, D. Sosnov, V. Sulimov, L. Uvarov, A. Vorobyev

Institute for Nuclear Research, Moscow, Russia
Yu. Andreev, A. Dermenev, S. Gninenko, N. Golubev, A. Karneyeu, M. Kirsanov, N. Krasnikov, A. Pashenkov, D. Tlisov, A. Toropin

Institute for Theoretical and Experimental Physics named by A.I. Alikhanov of NRC 'Kurchatov Institute', Moscow, Russia
V. Epshteyn, V. Gavrilov, N. Lychkovskaya, A. Nikitenko[42], V. Popov, I. Pozdnyakov, G. Safronov, A. Spiridonov, A. Stepennov, M. Toms, E. Vlasov, A. Zhokin

Moscow Institute of Physics and Technology, Moscow, Russia
T. Aushev

National Research Nuclear University 'Moscow Engineering Physics Institute' (MEPhI), Moscow, Russia
M. Chadeeva[43], P. Parygin, D. Philippov, E. Popova, V. Rusinov

P.N. Lebedev Physical Institute, Moscow, Russia
V. Andreev, M. Azarkin, I. Dremin, M. Kirakosyan, A. Terkulov

Skobeltsyn Institute of Nuclear Physics, Lomonosov Moscow State University, Moscow, Russia
A. Baskakov, A. Belyaev, E. Boos, V. Bunichev, M. Dubinin[44], L. Dudko, V. Klyukhin, N. Korneeva, I. Lokhtin, S. Obraztsov, M. Perfilov, V. Savrin, P. Volkov

Novosibirsk State University (NSU), Novosibirsk, Russia
A. Barnyakov[45], V. Blinov[45], T. Dimova[45], L. Kardapoltsev[45], Y. Skovpen[45]

Institute for High Energy Physics of National Research Centre 'Kurchatov Institute', Protvino, Russia
I. Azhgirey, I. Bayshev, S. Bitioukov, V. Kachanov, D. Konstantinov, P. Mandrik, V. Petrov, R. Ryutin, S. Slabospitskii, A. Sobol, S. Troshin, N. Tyurin, A. Uzunian, A. Volkov

National Research Tomsk Polytechnic University, Tomsk, Russia
A. Babaev, A. Iuzhakov, V. Okhotnikov

Tomsk State University, Tomsk, Russia
V. Borchsh, V. Ivanchenko, E. Tcherniaev

University of Belgrade: Faculty of Physics and VINCA Institute of Nuclear Sciences
P. Adzic[46], P. Cirkovic, D. Devetak, M. Dordevic, P. Milenovic, J. Milosevic, M. Stojanovic

Centro de Investigaciones Energéticas Medioambientales y Tecnológicas (CIEMAT), Madrid, Spain
M. Aguilar-Benitez, J. Alcaraz Maestre, A. lvarez Fernández, I. Bachiller, M. Barrio Luna, J.A. Brochero Cifuentes, C.A. Carrillo Montoya, M. Cepeda, M. Cerrada, N. Colino, B. De La Cruz, A. Delgado Peris, C. Fernandez Bedoya, J.P. Fernández Ramos, J. Flix, M.C. Fouz, O. Gonzalez Lopez, S. Goy Lopez, J.M. Hernandez, M.I. Josa, D. Moran, . Navarro Tobar, A. Pérez-Calero Yzquierdo, J. Puerta Pelayo, I. Redondo, L. Romero, S. Sánchez Navas, M.S. Soares, A. Triossi, C. Willmott

Universidad Autónoma de Madrid, Madrid, Spain
C. Albajar, J.F. de Trocóniz

Universidad de Oviedo, Instituto Universitario de Ciencias y Tecnologías Espaciales de Asturias (ICTEA), Oviedo, Spain
B. Alvarez Gonzalez, J. Cuevas, C. Erice, J. Fernandez Menendez, S. Folgueras, I. Gonzalez Caballero, J.R. González Fernández, E. Palencia Cortezon, V. Rodríguez Bouza, S. Sanchez Cruz

Instituto de Física de Cantabria (IFCA), CSIC-Universidad de Cantabria, Santander, Spain
I.J. Cabrillo, A. Calderon, B. Chazin Quero, J. Duarte Campderros, M. Fernandez, P.J. Fernández Manteca, A. García Alonso, G. Gomez, C. Martinez Rivero, P. Martinez Ruiz del Arbol, F. Matorras, J. Piedra Gomez, C. Prieels, T. Rodrigo, A. Ruiz-Jimeno, L. Russo[47], L. Scodellaro, N. Trevisani, I. Vila, J.M. Vizan Garcia

University of Colombo, Colombo, Sri Lanka
K. Malagalage

University of Ruhuna, Department of Physics, Matara, Sri Lanka
W.G.D. Dharmaratna, N. Wickramage

CERN, European Organization for Nuclear Research, Geneva, Switzerland
D. Abbaneo, B. Akgun, E. Auffray, G. Auzinger, J. Baechler, P. Baillon, A.H. Ball, D. Barney, J. Bendavid, M. Bianco, A. Bocci, E. Bossini, C. Botta, E. Brondolin, T. Camporesi, A. Caratelli, G. Cerminara, E. Chapon, G. Cucciati, D. d'Enterria, A. Dabrowski, N. Daci, V. Daponte, A. David, O. Davignon, A. De Roeck, N. Deelen, M. Deile, M. Dobson, M. Dünser, N. Dupont, A. Elliott-Peisert, F. Fallavollita[48], D. Fasanella, G. Franzoni, J. Fulcher, W. Funk, S. Giani, D. Gigi, A. Gilbert, K. Gill, F. Glege, M. Gruchala, M. Guilbaud, D. Gulhan, J. Hegeman, C. Heidegger, Y. Iiyama, V. Innocente, P. Janot, O. Karacheban[21], J. Kaspar, J. Kieseler, M. Krammer[1], C. Lange, P. Lecoq, C. Lourenço, L. Malgeri, M. Mannelli, A. Massironi, F. Meijers, J.A. Merlin, S. Mersi, E. Meschi, F. Moortgat, M. Mulders, J. Ngadiuba, S. Nourbakhsh, S. Orfanelli, L. Orsini, F. Pantaleo[18], L. Pape, E. Perez, M. Peruzzi, A. Petrilli, G. Petrucciani, A. Pfeiffer, M. Pierini, F.M. Pitters, D. Rabady, A. Racz, M. Rovere, H. Sakulin, C. Schäfer, C. Schwick, M. Selvaggi, A. Sharma, P. Silva, W. Snoeys, P. Sphicas[49], J. Steggemann, V.R. Tavolaro, D. Treille, A. Tsirou, A. Vartak, M. Verzetti, W.D. Zeuner

Paul Scherrer Institut, Villigen, Switzerland
L. Caminada[50], K. Deiters, W. Erdmann, R. Horisberger, Q. Ingram, H.C. Kaestli, D. Kotlinski, U. Langenegger, T. Rohe, S.A. Wiederkehr

ETH Zurich - Institute for Particle Physics and Astrophysics (IPA), Zurich, Switzerland
M. Backhaus, P. Berger, N. Chernyavskaya, G. Dissertori, M. Dittmar, M. Donegà, C. Dorfer, T.A. Gómez Espinosa, C. Grab, D. Hits, T. Klijnsma, W. Lustermann, R.A. Manzoni, M. Marionneau, M.T. Meinhard, F. Micheli, P. Musella, F. Nessi-Tedaldi, F. Pauss, G. Perrin, L. Perrozzi, S. Pigazzini, M. Reichmann, C. Reissel, T. Reitenspiess, D. Ruini, D.A. Sanz Becerra, M. Schönenberger, L. Shchutska, M.L. Vesterbacka Olsson, R. Wallny, D.H. Zhu

Universität Zürich, Zurich, Switzerland
T.K. Aarrestad, C. Amsler[51], D. Brzhechko, M.F. Canelli, A. De Cosa, R. Del Burgo, S. Donato, B. Kilminster, S. Leontsinis, V.M. Mikuni, I. Neutelings, G. Rauco, P. Robmann, D. Salerno, K. Schweiger, C. Seitz, Y. Takahashi, S. Wertz, A. Zucchetta

National Central University, Chung-Li, Taiwan
T.H. Doan, C.M. Kuo, W. Lin, S.S. Yu

National Taiwan University (NTU), Taipei, Taiwan
P. Chang, Y. Chao, K.F. Chen, P.H. Chen, W.-S. Hou, Y.y. Li, R.-S. Lu, E. Paganis, A. Psallidas, A. Steen

Chulalongkorn University, Faculty of Science, Department of Physics, Bangkok, Thailand
B. Asavapibhop, C. Asawatangtrakuldee, N. Srimanobhas, N. Suwonjandee

ukurova University, Physics Department, Science and Art Faculty, Adana, Turkey
M.N. Bakirci[52], A. Bat, F. Boran, S. Damarseckin[53], Z.S. Demiroglu, F. Dolek, C. Dozen, I. Dumanoglu, EmineGurpinar Guler[54], Y. Guler, I. Hos[55], C. Isik, E.E. Kangal[56], O. Kara, A. Kayis Topaksu, U. Kiminsu, M. Oglakci, G. Onengut, K. Ozdemir[57], S. Ozturk[52], A.E. Simsek, D. Sunar Cerci[58], U.G. Tok, H. Topakli[52], S. Turkcapar, I.S. Zorbakir, C. Zorbilmez

Middle East Technical University, Physics Department, Ankara, Turkey
B. Isildak[59], G. Karapinar[60], M. Yalvac

Bogazici University, Istanbul, Turkey
I.O. Atakisi, E. Gülmez, M. Kaya[61], O. Kaya[62], B. Kaynak, Ö. Özçelik, S. Ozkorucuklu[63], S. Tekten, E.A. Yetkin[64]

Istanbul Technical University, Istanbul, Turkey
A. Cakir, K. Cankocak, Y. Komurcu, S. Sen[65]

Institute for Scintillation Materials of National Academy of Science of Ukraine, Kharkov, Ukraine
B. Grynyov

National Scientific Center, Kharkov Institute of Physics and Technology, Kharkov, Ukraine
L. Levchuk

University of Bristol, Bristol, United Kingdom
F. Ball, E. Bhal, S. Bologna, J.J. Brooke, D. Burns, E. Clement, D. Cussans, H. Flacher, J. Goldstein, G.P. Heath, H.F. Heath, L. Kreczko, S. Paramesvaran, B. Penning, T. Sakuma, S. Seif El Nasr-Storey, D. Smith, V.J. Smith, J. Taylor, A. Titterton

Rutherford Appleton Laboratory, Didcot, United Kingdom
K.W. Bell, A. Belyaev[66], C. Brew, R.M. Brown, D. Cieri, D.J.A. Cockerill, J.A. Coughlan, K. Harder, S. Harper, J. Linacre, K. Manolopoulos, D.M. Newbold, E. Olaiya, D. Petyt, T. Reis, T. Schuh, C.H. Shepherd-Themistocleous, A. Thea, I.R. Tomalin, T. Williams, W.J. Womersley

Imperial College, London, United Kingdom
R. Bainbridge, P. Bloch, J. Borg, S. Breeze, O. Buchmuller, A. Bundock, GurpreetSingh CHAHAL[67], D. Colling, P. Dauncey, G. Davies, M. Della Negra, R. Di Maria, P. Everaerts, G. Hall, G. Iles, T. James, M. Komm, C. Laner, L. Lyons, A.-M. Magnan, S. Malik, A. Martelli, V. Milosevic, J. Nash[68], V. Palladino, M. Pesaresi, D.M. Raymond, A. Richards, A. Rose, E. Scott, C. Seez, A. Shtipliyski, M. Stoye, T. Strebler, S. Summers, A. Tapper, K. Uchida, T. Virdee[18], N. Wardle, D. Winterbottom, J. Wright, A.G. Zecchinelli, S.C. Zenz

Brunel University, Uxbridge, United Kingdom
J.E. Cole, P.R. Hobson, A. Khan, P. Kyberd, C.K. Mackay, A. Morton, I.D. Reid, L. Teodorescu, S. Zahid

Baylor University, Waco, USA
K. Call, J. Dittmann, K. Hatakeyama, C. Madrid, B. McMaster, N. Pastika, C. Smith

Catholic University of America, Washington, DC, USA
R. Bartek, A. Dominguez, R. Uniyal

The University of Alabama, Tuscaloosa, USA
A. Buccilli, S.I. Cooper, C. Henderson, P. Rumerio, C. West

Boston University, Boston, USA
D. Arcaro, T. Bose, Z. Demiragli, D. Gastler, S. Girgis, D. Pinna, C. Richardson, J. Rohlf, D. Sperka, I. Suarez, L. Sulak, D. Zou

Brown University, Providence, USA
G. Benelli, B. Burkle, X. Coubez, D. Cutts, Y.t. Duh, M. Hadley, J. Hakala, U. Heintz, J.M. Hogan[69], K.H.M. Kwok, E. Laird, G. Landsberg, J. Lee, Z. Mao, M. Narain, S. Sagir[70], R. Syarif, E. Usai, D. Yu

University of California, Davis, Davis, USA
R. Band, C. Brainerd, R. Breedon, M. Calderon De La Barca Sanchez, M. Chertok, J. Conway, R. Conway, P.T. Cox, R. Erbacher, C. Flores, G. Funk, F. Jensen, W. Ko, O. Kukral, R. Lander, M. Mulhearn, D. Pellett, J. Pilot, M. Shi, D. Stolp, D. Taylor, K. Tos, M. Tripathi, Z. Wang, F. Zhang

University of California, Los Angeles, USA
M. Bachtis, C. Bravo, R. Cousins, A. Dasgupta, A. Florent, J. Hauser, M. Ignatenko, N. Mccoll, W.A. Nash, S. Regnard, D. Saltzberg, C. Schnaible, B. Stone, V. Valuev

University of California, Riverside, Riverside, USA
K. Burt, R. Clare, J.W. Gary, S.M.A. Ghiasi Shirazi, G. Hanson, G. Karapostoli, E. Kennedy, O.R. Long, M. Olmedo Negrete, M.I. Paneva, W. Si, L. Wang, H. Wei, S. Wimpenny, B.R. Yates, Y. Zhang

University of California, San Diego, La Jolla, USA
J.G. Branson, P. Chang, S. Cittolin, M. Derdzinski, R. Gerosa, D. Gilbert, B. Hashemi, D. Klein, V. Krutelyov, J. Letts, M. Masciovecchio, S. May, S. Padhi, M. Pieri, V. Sharma, M. Tadel, F. Würthwein, A. Yagil, G. Zevi Della Porta

University of California, Santa Barbara - Department of Physics, Santa Barbara, USA
N. Amin, R. Bhandari, C. Campagnari, M. Citron, V. Dutta, M. Franco Sevilla, L. Gouskos, J. Incandela, B. Marsh, H. Mei, A. Ovcharova, H. Qu, J. Richman, U. Sarica, D. Stuart, S. Wang, J. Yoo

California Institute of Technology, Pasadena, USA
D. Anderson, A. Bornheim, J.M. Lawhorn, N. Lu, H.B. Newman, T.Q. Nguyen, J. Pata, M. Spiropulu, J.R. Vlimant, S. Xie, Z. Zhang, R.Y. Zhu

Carnegie Mellon University, Pittsburgh, USA
M.B. Andrews, T. Ferguson, T. Mudholkar, M. Paulini, M. Sun, I. Vorobiev, M. Weinberg

University of Colorado Boulder, Boulder, USA
J.P. Cumalat, W.T. Ford, A. Johnson, E. MacDonald, T. Mulholland, R. Patel, A. Perloff, K. Stenson, K.A. Ulmer, S.R. Wagner

Cornell University, Ithaca, USA
J. Alexander, J. Chaves, Y. Cheng, J. Chu, A. Datta, A. Frankenthal, K. Mcdermott, N. Mirman, J.R. Patterson, D. Quach, A. Rinkevicius[71], A. Ryd, S.M. Tan, Z. Tao, J. Thom, P. Wittich, M. Zientek

Fermi National Accelerator Laboratory, Batavia, USA
S. Abdullin, M. Albrow, M. Alyari, G. Apollinari, A. Apresyan, A. Apyan, S. Banerjee, L.A.T. Bauerdick, A. Beretvas, J. Berryhill, P.C. Bhat, K. Burkett, J.N. Butler, A. Canepa, G.B. Cerati, H.W.K. Cheung, F. Chlebana, M. Cremonesi, J. Duarte, V.D. Elvira, J. Freeman, Z. Gecse, E. Gottschalk, L. Gray, D. Green, S. Grünendahl, O. Gutsche, AllisonReinsvold Hall,

J. Hanlon, R.M. Harris, S. Hasegawa, R. Heller, J. Hirschauer, B. Jayatilaka, S. Jindariani, M. Johnson, U. Joshi, B. Klima, M.J. Kortelainen, B. Kreis, S. Lammel, J. Lewis, D. Lincoln, R. Lipton, M. Liu, T. Liu, J. Lykken, K. Maeshima, J.M. Marraffino, D. Mason, P. McBride, P. Merkel, S. Mrenna, S. Nahn, V. O'Dell, V. Papadimitriou, K. Pedro, C. Pena, G. Rakness, F. Ravera, L. Ristori, B. Schneider, E. Sexton-Kennedy, N. Smith, A. Soha, W.J. Spalding, L. Spiegel, S. Stoynev, J. Strait, N. Strobbe, L. Taylor, S. Tkaczyk, N.V. Tran, L. Uplegger, E.W. Vaandering, C. Vernieri, M. Verzocchi, R. Vidal, M. Wang, H.A. Weber

University of Florida, Gainesville, USA
D. Acosta, P. Avery, P. Bortignon, D. Bourilkov, A. Brinkerhoff, L. Cadamuro, A. Carnes, V. Cherepanov, D. Curry, F. Errico, R.D. Field, S.V. Gleyzer, B.M. Joshi, M. Kim, J. Konigsberg, A. Korytov, K.H. Lo, P. Ma, K. Matchev, N. Menendez, G. Mitselmakher, D. Rosenzweig, K. Shi, J. Wang, S. Wang, X. Zuo

Florida International University, Miami, USA
Y.R. Joshi

Florida State University, Tallahassee, USA
T. Adams, A. Askew, S. Hagopian, V. Hagopian, K.F. Johnson, R. Khurana, T. Kolberg, G. Martinez, T. Perry, H. Prosper, C. Schiber, R. Yohay, J. Zhang

Florida Institute of Technology, Melbourne, USA
M.M. Baarmand, V. Bhopatkar, M. Hohlmann, D. Noonan, M. Rahmani, M. Saunders, F. Yumiceva

University of Illinois at Chicago (UIC), Chicago, USA
M.R. Adams, L. Apanasevich, D. Berry, R.R. Betts, R. Cavanaugh, X. Chen, S. Dittmer, O. Evdokimov, C.E. Gerber, D.A. Hangal, D.J. Hofman, K. Jung, C. Mills, T. Roy, M.B. Tonjes, N. Varelas, H. Wang, X. Wang, Z. Wu

The University of Iowa, Iowa City, USA
M. Alhusseini, B. Bilki[54], W. Clarida, K. Dilsiz[72], S. Durgut, R.P. Gandrajula, M. Haytmyradov, V. Khristenko, O.K. Köseyan, J.-P. Merlo, A. Mestvirishvili[73], A. Moeller, J. Nachtman, H. Ogul[74], Y. Onel, F. Ozok[75], A. Penzo, C. Snyder, E. Tiras, J. Wetzel

Johns Hopkins University, Baltimore, USA
B. Blumenfeld, A. Cocoros, N. Eminizer, D. Fehling, L. Feng, A.V. Gritsan, W.T. Hung, P. Maksimovic, J. Roskes, M. Swartz, M. Xiao

The University of Kansas, Lawrence, USA
C. Baldenegro Barrera, P. Baringer, A. Bean, S. Boren, J. Bowen, A. Bylinkin, T. Isidori, S. Khalil, J. King, G. Krintiras, A. Kropivnitskaya, C. Lindsey, D. Majumder, W. Mcbrayer, N. Minafra, M. Murray, C. Rogan, C. Royon, S. Sanders, E. Schmitz, J.D. Tapia Takaki, Q. Wang, J. Williams, G. Wilson

Kansas State University, Manhattan, USA
S. Duric, A. Ivanov, K. Kaadze, D. Kim, Y. Maravin, D.R. Mendis, T. Mitchell, A. Modak, A. Mohammadi

Lawrence Livermore National Laboratory, Livermore, USA
F. Rebassoo, D. Wright

University of Maryland, College Park, USA
A. Baden, O. Baron, A. Belloni, S.C. Eno, Y. Feng, N.J. Hadley, S. Jabeen, G.Y. Jeng, R.G. Kellogg,

J. Kunkle, A.C. Mignerey, S. Nabili, F. Ricci-Tam, M. Seidel, Y.H. Shin, A. Skuja, S.C. Tonwar, K. Wong

Massachusetts Institute of Technology, Cambridge, USA
D. Abercrombie, B. Allen, A. Baty, R. Bi, S. Brandt, W. Busza, I.A. Cali, M. D'Alfonso, G. Gomez Ceballos, M. Goncharov, P. Harris, D. Hsu, M. Hu, M. Klute, D. Kovalskyi, Y.-J. Lee, P.D. Luckey, B. Maier, A.C. Marini, C. Mcginn, C. Mironov, S. Narayanan, X. Niu, C. Paus, D. Rankin, C. Roland, G. Roland, Z. Shi, G.S.F. Stephans, K. Sumorok, K. Tatar, D. Velicanu, J. Wang, T.W. Wang, B. Wyslouch

University of Minnesota, Minneapolis, USA
A.C. Benvenuti[†], R.M. Chatterjee, A. Evans, S. Guts, P. Hansen, J. Hiltbrand, Sh. Jain, S. Kalafut, Y. Kubota, Z. Lesko, J. Mans, R. Rusack, M.A. Wadud

University of Mississippi, Oxford, USA
J.G. Acosta, S. Oliveros

University of Nebraska-Lincoln, Lincoln, USA
K. Bloom, D.R. Claes, C. Fangmeier, L. Finco, F. Golf, R. Gonzalez Suarez, R. Kamalieddin, I. Kravchenko, J.E. Siado, G.R. Snow, B. Stieger

State University of New York at Buffalo, Buffalo, USA
G. Agarwal, C. Harrington, I. Iashvili, A. Kharchilava, C. Mclean, D. Nguyen, A. Parker, J. Pekkanen, S. Rappoccio, B. Roozbahani

Northeastern University, Boston, USA
G. Alverson, E. Barberis, C. Freer, Y. Haddad, A. Hortiangtham, G. Madigan, D.M. Morse, T. Orimoto, L. Skinnari, A. Tishelman-Charny, T. Wamorkar, B. Wang, A. Wisecarver, D. Wood

Northwestern University, Evanston, USA
S. Bhattacharya, J. Bueghly, T. Gunter, K.A. Hahn, N. Odell, M.H. Schmitt, K. Sung, M. Trovato, M. Velasco

University of Notre Dame, Notre Dame, USA
R. Bucci, N. Dev, R. Goldouzian, M. Hildreth, K. Hurtado Anampa, C. Jessop, D.J. Karmgard, K. Lannon, W. Li, N. Loukas, N. Marinelli, I. Mcalister, F. Meng, C. Mueller, Y. Musienko[37], M. Planer, R. Ruchti, P. Siddireddy, G. Smith, S. Taroni, M. Wayne, A. Wightman, M. Wolf, A. Woodard

The Ohio State University, Columbus, USA
J. Alimena, B. Bylsma, L.S. Durkin, S. Flowers, B. Francis, C. Hill, W. Ji, A. Lefeld, T.Y. Ling, B.L. Winer

Princeton University, Princeton, USA
S. Cooperstein, G. Dezoort, P. Elmer, J. Hardenbrook, N. Haubrich, S. Higginbotham, A. Kalogeropoulos, S. Kwan, D. Lange, M.T. Lucchini, J. Luo, D. Marlow, K. Mei, I. Ojalvo, J. Olsen, C. Palmer, P. Piroué, J. Salfeld-Nebgen, D. Stickland, C. Tully, Z. Wang

University of Puerto Rico, Mayaguez, USA
S. Malik, S. Norberg

Purdue University, West Lafayette, USA
A. Barker, V.E. Barnes, S. Das, L. Gutay, M. Jones, A.W. Jung, A. Khatiwada, B. Mahakud, D.H. Miller, G. Negro, N. Neumeister, C.C. Peng, S. Piperov, H. Qiu, J.F. Schulte, J. Sun, F. Wang, R. Xiao, W. Xie

Purdue University Northwest, Hammond, USA
T. Cheng, J. Dolen, N. Parashar

Rice University, Houston, USA
K.M. Ecklund, S. Freed, F.J.M. Geurts, M. Kilpatrick, Arun Kumar, W. Li, B.P. Padley, R. Redjimi, J. Roberts, J. Rorie, W. Shi, A.G. Stahl Leiton, Z. Tu, A. Zhang

University of Rochester, Rochester, USA
A. Bodek, P. de Barbaro, R. Demina, J.L. Dulemba, C. Fallon, T. Ferbel, M. Galanti, A. Garcia-Bellido, J. Han, O. Hindrichs, A. Khukhunaishvili, E. Ranken, P. Tan, R. Taus

Rutgers, The State University of New Jersey, Piscataway, USA
B. Chiarito, J.P. Chou, A. Gandrakota, Y. Gershtein, E. Halkiadakis, A. Hart, M. Heindl, E. Hughes, S. Kaplan, S. Kyriacou, I. Laflotte, A. Lath, R. Montalvo, K. Nash, M. Osherson, H. Saka, S. Salur, S. Schnetzer, D. Sheffield, S. Somalwar, R. Stone, S. Thomas, P. Thomassen

University of Tennessee, Knoxville, USA
H. Acharya, A.G. Delannoy, J. Heideman, G. Riley, S. Spanier

Texas A&M University, College Station, USA
O. Bouhali[76], A. Celik, M. Dalchenko, M. De Mattia, A. Delgado, S. Dildick, R. Eusebi, J. Gilmore, T. Huang, T. Kamon[77], S. Luo, D. Marley, R. Mueller, D. Overton, L. Perniè, D. Rathjens, A. Safonov

Texas Tech University, Lubbock, USA
N. Akchurin, J. Damgov, F. De Guio, S. Kunori, K. Lamichhane, S.W. Lee, T. Mengke, S. Muthumuni, T. Peltola, S. Undleeb, I. Volobouev, Z. Wang, A. Whitbeck

Vanderbilt University, Nashville, USA
S. Greene, A. Gurrola, R. Janjam, W. Johns, C. Maguire, A. Melo, H. Ni, K. Padeken, F. Romeo, P. Sheldon, S. Tuo, J. Velkovska, M. Verweij

University of Virginia, Charlottesville, USA
M.W. Arenton, P. Barria, B. Cox, G. Cummings, R. Hirosky, M. Joyce, A. Ledovskoy, C. Neu, B. Tannenwald, Y. Wang, E. Wolfe, F. Xia

Wayne State University, Detroit, USA
R. Harr, P.E. Karchin, N. Poudyal, J. Sturdy, P. Thapa, S. Zaleski

University of Wisconsin - Madison, Madison, WI, USA
J. Buchanan, C. Caillol, D. Carlsmith, S. Dasu, I. De Bruyn, L. Dodd, F. Fiori, C. Galloni, B. Gomber[78], M. Herndon, A. Hervé, U. Hussain, P. Klabbers, A. Lanaro, A. Loeliger, K. Long, R. Loveless, J. Madhusudanan Sreekala, T. Ruggles, A. Savin, V. Sharma, W.H. Smith, D. Teague, S. Trembath-reichert, N. Woods

†: Deceased
1: Also at Vienna University of Technology, Vienna, Austria
2: Also at IRFU, CEA, Université Paris-Saclay, Gif-sur-Yvette, France
3: Also at Universidade Estadual de Campinas, Campinas, Brazil
4: Also at Federal University of Rio Grande do Sul, Porto Alegre, Brazil
5: Also at UFMS, Nova Andradina, Brazil
6: Also at Universidade Federal de Pelotas, Pelotas, Brazil
7: Also at Université Libre de Bruxelles, Bruxelles, Belgium
8: Also at University of Chinese Academy of Sciences, Beijing, China
9: Also at Institute for Theoretical and Experimental Physics named by A.I. Alikhanov of NRC

‘Kurchatov Institute’, Moscow, Russia
10: Also at Joint Institute for Nuclear Research, Dubna, Russia
11: Also at Cairo University, Cairo, Egypt
12: Also at Helwan University, Cairo, Egypt
13: Now at Zewail City of Science and Technology, Zewail, Egypt
14: Also at Purdue University, West Lafayette, USA
15: Also at Université de Haute Alsace, Mulhouse, France
16: Also at Tbilisi State University, Tbilisi, Georgia
17: Also at Erzincan Binali Yildirim University, Erzincan, Turkey
18: Also at CERN, European Organization for Nuclear Research, Geneva, Switzerland
19: Also at RWTH Aachen University, III. Physikalisches Institut A, Aachen, Germany
20: Also at University of Hamburg, Hamburg, Germany
21: Also at Brandenburg University of Technology, Cottbus, Germany
22: Also at Institute of Physics, University of Debrecen, Debrecen, Hungary, Debrecen, Hungary
23: Also at Institute of Nuclear Research ATOMKI, Debrecen, Hungary
24: Also at MTA-ELTE Lendület CMS Particle and Nuclear Physics Group, Eötvös Loránd University, Budapest, Hungary, Budapest, Hungary
25: Also at IIT Bhubaneswar, Bhubaneswar, India, Bhubaneswar, India
26: Also at Institute of Physics, Bhubaneswar, India
27: Also at Shoolini University, Solan, India
28: Also at University of Visva-Bharati, Santiniketan, India
29: Also at Isfahan University of Technology, Isfahan, Iran
30: Also at Italian National Agency for New Technologies, Energy and Sustainable Economic Development, Bologna, Italy
31: Also at Centro Siciliano di Fisica Nucleare e di Struttura Della Materia, Catania, Italy
32: Also at Scuola Normale e Sezione dell’INFN, Pisa, Italy
33: Also at Riga Technical University, Riga, Latvia, Riga, Latvia
34: Also at Malaysian Nuclear Agency, MOSTI, Kajang, Malaysia
35: Also at Consejo Nacional de Ciencia y Tecnología, Mexico City, Mexico
36: Also at Warsaw University of Technology, Institute of Electronic Systems, Warsaw, Poland
37: Also at Institute for Nuclear Research, Moscow, Russia
38: Now at National Research Nuclear University ’Moscow Engineering Physics Institute’ (MEPhI), Moscow, Russia
39: Also at Institute of Nuclear Physics of the Uzbekistan Academy of Sciences, Tashkent, Uzbekistan
40: Also at St. Petersburg State Polytechnical University, St. Petersburg, Russia
41: Also at University of Florida, Gainesville, USA
42: Also at Imperial College, London, United Kingdom
43: Also at P.N. Lebedev Physical Institute, Moscow, Russia
44: Also at California Institute of Technology, Pasadena, USA
45: Also at Budker Institute of Nuclear Physics, Novosibirsk, Russia
46: Also at Faculty of Physics, University of Belgrade, Belgrade, Serbia
47: Also at Università degli Studi di Siena, Siena, Italy
48: Also at INFN Sezione di Pavia [a], Università di Pavia [b], Pavia, Italy, Pavia, Italy
49: Also at National and Kapodistrian University of Athens, Athens, Greece
50: Also at Universität Zürich, Zurich, Switzerland
51: Also at Stefan Meyer Institute for Subatomic Physics, Vienna, Austria, Vienna, Austria
52: Also at Gaziosmanpasa University, Tokat, Turkey

53: Also at Şırnak University, Sirnak, Turkey
54: Also at Beykent University, Istanbul, Turkey, Istanbul, Turkey
55: Also at Istanbul Aydin University, Istanbul, Turkey
56: Also at Mersin University, Mersin, Turkey
57: Also at Piri Reis University, Istanbul, Turkey
58: Also at Adiyaman University, Adiyaman, Turkey
59: Also at Ozyegin University, Istanbul, Turkey
60: Also at Izmir Institute of Technology, Izmir, Turkey
61: Also at Marmara University, Istanbul, Turkey
62: Also at Kafkas University, Kars, Turkey
63: Also at Istanbul University, Istanbul, Turkey
64: Also at Istanbul Bilgi University, Istanbul, Turkey
65: Also at Hacettepe University, Ankara, Turkey
66: Also at School of Physics and Astronomy, University of Southampton, Southampton, United Kingdom
67: Also at IPPP Durham University, Durham, United Kingdom
68: Also at Monash University, Faculty of Science, Clayton, Australia
69: Also at Bethel University, St. Paul, Minneapolis, USA, St. Paul, USA
70: Also at Karamanoğlu Mehmetbey University, Karaman, Turkey
71: Also at Vilnius University, Vilnius, Lithuania
72: Also at Bingol University, Bingol, Turkey
73: Also at Georgian Technical University, Tbilisi, Georgia
74: Also at Sinop University, Sinop, Turkey
75: Also at Mimar Sinan University, Istanbul, Istanbul, Turkey
76: Also at Texas A&M University at Qatar, Doha, Qatar
77: Also at Kyungpook National University, Daegu, Korea, Daegu, Korea
78: Also at University of Hyderabad, Hyderabad, India